Chapter 2
Biosensors and Sensor Systems

Danny O'Hare

2.1 Introduction

This chapter is concerned with the design and operation of devices for the measurement of chemical concentrations in living systems. Whilst the meaning of chemical sensors has been somewhat broadened in recent years, a useful definition from a recent authoritative review [1] is: "*chemical sensors are miniaturised analytical devices that can deliver real time and online information on the presence of specific compounds or ions in complex samples*". Historically, a useful distinction was made between chemical sensors and biosensors in that a biosensor used a biologically derived element (enzyme, antibody, cell, tissue sample etc.) as part of the transduction process. This useful distinction has now been lost; *biosensor* is now often applied to any sensor measuring a chemical concentration in a biological system. Jiri Janata makes a further distinction between sensors and sensor systems, sensors being capable of continuous monitoring and sensor systems providing measurements in discrete steps. Turner, in a recent tutorial review [2] identifies two broad categories of device described under the heading 'biosensor': sophisticated and high-throughput lab-based instrumentation for rapid and accurate analysis of complex biological interactions and components, and portable easy-to-use devices for non-expert use, out of the lab, in the home or in a field environment, 'point-of-care' devices. This chapter will describe both chemical and biosensor (in the historical sense) approaches to the identification and quantification of chemical species in living systems and describe both sensors and sensor systems as described above. It will also outline recent developments, notably new materials with great potential for sensor applications. The underlying principles of the most widely used sensor types are described to enable their proper operation, design of

D. O'Hare (✉)
Department of Bioengineering, Imperial College London, London SW7 2BY, UK
e-mail: d.ohare@imperial.ac.uk

G.-Z. Yang (ed.), *Body Sensor Networks*, DOI 10.1007/978-1-4471-6374-9_2,

control instrumentation, optimisation of sensor design and correct interpretation of the resulting data. Exemplar applications are given to illustrate these principles.

Whilst development and application of chemical sensor and biosensor technology have been major research activities for decades, demographic and economic pressures in the developed world have provided an increased market pull and new opportunities for research and technology. Advances in medical science have coincided with increased life expectancy, a substantial concomitant increase in the proportion of elderly people in the population and massive improvements in the treatment and management of diseases associated with old age. Regardless of the healthcare economics, it is highly likely that there will simply be an insufficient amount of young people to meet the medical and clinical needs of the elderly. Furthermore, as has been demonstrated in the case of Type 1 diabetes, more frequent monitoring, especially outside the clinical environment, leads to an improved quality of life, fewer demands on acute healthcare and lower incidence of the vascular complications associated with diabetes in the long term. Blood glucose monitoring remains an important market, accounting for 85 % of all biosensor sales. Turner [2] claims that around $100 million is required to bring a device to market, given the investment required in high technology plant. At the moment, only blood glucose and pregnancy testing has the volume to attract this level of investment and just four companies (Abbott, Bayer, Roche and Johnson & Johnson) take more than 90 % of the blood glucose market.

The setting for sensor use dramatically alters both the healthcare economics and the technological challenges: it makes a huge difference whether the device is to be operated by a lay person, possibly the patient herself, or by a healthcare professional. Aside from personal use, the most obvious application is in critical care monitoring. The requirements for sensors in critical care have been usefully reviewed by Moore et al. [3]. The rather optimistic wish list is summarised below:

- An accurate and stable sensor for an essential variable; it must be accurate and stable indefinitely. Physicochemical detection must be reversible to minimise sensor recovery and response times;
- Non- or minimally-invasive;
- Continuous monitoring function with the ability to display trends;
- Easy to use and a display that is easily understood;
- Small size and weight;
- Ruggedness and transportability.

In addition to the rather challenging engineering specifications, Moore also points out that the economic value of continuous monitoring has not yet been demonstrated.

An important additional driver is the increased realisation that individual patient responses to drug therapy can vary greatly. This is a particularly acute problem in cancer chemotherapy where time is obviously pressing, but can be important in chronic management of a host of conditions. For example, the widespread use of statins in the management of atherosclerosis and cardiovascular disease is hindered by idiosyncratic adverse effects including myositis and myopathy and, rarely, rhabdomyolysis. Such variable responses to drug therapy in many cases are believed to be due to underlying genetic differences. Rapid identification of an

individual patient's "ideal drug" is therefore important and provides a further application for sensor technology.

Before beginning an exposition of the basic science and technology underpinning sensor design, some overview of the motivations and unique problems posed by biological systems is required.

2.2 Bioanalysis

Recent decades have seen rapid developments and great technological achievements in bioanalysis including the sequencing of the entire human genome. Though the dream was to produce biology's equivalent of the periodic table of the elements [4, 5], the situation has turned out to be more complex. The somewhat surprising discovery of the relatively small number of genes (around 30,000) and the growing realisation of the complex networks involved have resulted in fewer direct applications to human health than originally anticipated. Nonetheless, there has been real insight, which is certain to inform healthcare and likely to lead to new opportunities for medical devices. Proteomics and metabolomics [6] have similarly improved understanding of physiological and metabolic pathways at the cellular level and have led to a more quantitative engineering approach – systems biology – which has the potential to give a quantitative functional understanding of the repertoire of cellular behaviour. DNA sequencing is becoming faster and cheaper with each passing year and new technology on the horizon – particularly nanopore devices – hold out great promise for better fundamental understanding of cellular function in health and disease and also provide great opportunities for personalised medicine. All of these approaches are likely to provide new approaches to drug discovery [7, 8], lead compound identification [9] and to inform personalised approaches to drug therapy [10].

Bioanalysis presents several important problems to the analytical scientist. These range from the difficulty in correctly identifying the research question to more mundane but nonetheless technically challenging issues around materials, stability and calibration. The first problem is to identify the motivation for measuring chemical concentrations.

This field is essentially multidisciplinary, and technical terminology regrettably differs between the different traditional disciplines that contribute to sensor research. This chapter follows the conventions of analytical science, and key jargon is defined below:

2.2.1 Some Jargon

- ***Analyte:*** the target molecular species. This is the molecule we wish to identify and quantify.
- ***Matrix:*** everything else present in our sample apart from the analyte. Matrix interference, where sensor response is inadvertently elicited by so-called

spectator species present in the sample, is a major problem in bioanalysis due to the complexity of biological systems. Matrix interference can usefully be divided into two categories: (i) signal caused by non-target molecules, e.g., ascorbic acid or paracetamol, both of which are oxidized at potentials used for the measurement of glucose, and (ii) sensor inactivation or 'poisoning' due to adsorption of proteins or other surface-active material. For example, albumin is typically present at around 4 % (w/v) in plasma. Adsorption of albumin can occlude or scatter light transmission from fibre optic sensors or prevent electrocatalysis on amperometric or voltammetric sensors (*vide infra*).

- ***Sensitivity:*** the change in sensor output per unit change in analyte concentration. This could be measured in μA mol^{-1} dm^3 for an amperometric biosensor or absorbance units per mole for a spectrometric device.
- ***Limit of Detection (LOD):*** the level of analyte that leads to a sensor signal which is statistically significantly different from the background signal obtained in the absence of analyte. A frequently used definition of LOD is a concentration that gives a signal greater than three times the standard deviation of a blank sample consisting entirely of matrix. This can often be most easily calculated from a calibration-working curve, as the concentration is equivalent to three times the standard deviation of the ordinal intercept. A signal at LOD cannot be related to a specific concentration and can only infer that the target analyte is present, to a given probability, i.e., the sensor is not merely giving out noise. If a numerical concentration is required, the limit of quantitation must be defined, and is typically five times higher than the LOD. Standard deviation of the background is an essential specification of any sensor as this can be applied, multiplied by a suitable coverage factor, by any user according to their needs.
- ***Selectivity:*** the ability of the analytical method to respond only to the target analyte. Strict determination of selectivity is frequently a problem in bioanalysis where the real instantaneous composition of the sample cannot be determined in practice. The expected error can be quantified for each expected interferent as:

$$Maximum\ \ error = \frac{Effect\ \ of\ \ interferent}{Effect\ \ of\ \ analyte} \times 100\% \tag{2.1}$$

where the interferent concentration is maximum expected in the sample and the analyte concentration is the minimum expected. Where there are more than one expected interferents, these can be summed (assuming no synergistic effects). This approach works well for well-characterised analytes such as human blood samples where the composition is relatively well known from decades of measurements over millions of individuals. It is disappointing that relatively few published papers take the trouble to calculate this key parameter, which is obviously essential in determining fitness for purpose. Where sufficient data is available to enable its calculation, the result is frequently disappointing for the aspirant investigator.

Other key parameters are response times (usually quantified as 10–90 % response time to a step change in concentration, or the time constant of a presumed monoexponential response to a step change in concentration) and, frequently ignored, the recovery time or reversibility of response. Rapid reversibility is usually a contradictory requirement to high selectivity due to the nature of the interactions involved; molecular level selectivity typically requires the analyte to approach within a bond length of the sensor.

2.2.2 *Bioanalysis – What Does Chemical Concentration Mean in Biology?*

Concepts of chemical concentration – the amount of material either by mass, moles or number of particles per unit volume – derive from chemistry which takes place typically in volumes of cm^3 and upwards with at least concentrations that are millimolar. We are, therefore, typically considering at least 10^{16} particles, and statistical fluctuations from one region to another are negligible. Concepts based on the essentially homogeneous nature of such solutions translate poorly to biology where heterogeneity and compartmentalisation exist on every length scale from the whole organism down to the subcellular domain. Cells are only able to sense and respond to their immediate environment. A typical mammalian cell is around 10 μm in diameter and if the target analyte concentration is sub nanomolar, which is frequently the case, then fewer than 1,000 molecules will be present. Under these circumstances, assumptions of homogeneity and the law of mass action simply cannot be valid. We would expect, and indeed do find, considerable variations in concentration when measuring at the level of single cells. Some of this variation must be due to natural biological variation (cells are not mass produced according to six sigma processes!) but, inevitably, much of the variation must be due to stochastic variations in the number of signalling molecules detected by the cells themselves.

A further complication is that many biologically significant molecules are produced and consumed at discrete locations (membrane bound enzymes and transporter proteins), which are small even on the length scale of the single cell. The precise *concentration* recorded will depend heavily on the precise position and the sampling volume. In living creatures it is usually not possible to be sure which part of the plume of concentration the sensor is responding to. Heterogeneity and localised sources and sinks greatly complicate the interpretation of concentration data which, for in vivo measurement requires prior definition of the length scale of interest and engineered devices that can deliver the appropriate resolution.

A key decision that the scientist needs to take is whether to attempt the measurement in situ, on-the-fly in real time or to remove what one hopes is a representative sample and preserve it for more leisurely analysis under more controlled conditions. In situ measurements in the physiological system can be

both influenced by and influence the response to the measurement device or probe. The immune system will normally mount a foreign body response [11], initially consisting of protein (and other biomolecule) deposition, which can impair device function. Fibrous capsule formation may seal off the measurement device over a period of several hours to several days and acute inflammatory responses may mean that the results are dominated by the effects of the measurement itself. Some methods of separation of the biological analytes can therefore be a potentially simplifying procedure in bioanalysis and for point-of-care applications; lab-chip devices are obviously attractive options [12].

Rapid response times are also required in vivo due to the time varying concentrations arising from continuous interactions in the system. Good temporal resolution is frequently inimical to stability and noise rejection and optimisation is always necessary. In contrast, the *ex situ* experiment requires isolation and preservation of the sample. Such destructive analysis necessarily limits the sample size – there are absolute limits of sample size if the patient is to survive the measurement.

Limited sample size is an important motivation for the development of miniaturised systems. Separation, clean-up and the preparation of, usually, a homogeneous solution greatly simplifies the chemical measurement step, though preserving the integrity of the sample and ensuring that analyte recovery is high and consistent are not trivial engineering challenges. However, the problems of the representative sample and the relevance to the underlying physiology remain. The conventional analytical approaches of using certified reference materials or standard solutions to validate the analytical measurement and the individual steps often cannot be applied to the overall process. Standard addition may be possible on isolated tissue, but usually cannot be attempted on a living organism.

In summary, there are typically three motivations for measuring chemical concentrations in living systems: (i) statistical correlation with expensive history-taking or known disease condition as an aid to diagnosis, for example rapid detection and quantification of known biomarkers; (ii) legal requirements, such as the strict limits on blood-alcohol levels for driving in most jurisdictions and (iii) fundamental research in physiology and biochemistry. Whilst the specifications for (i) and (ii) are relatively straightforward, new devices and new understanding of physiology require an essentially collaborative approach between clinicians, biologists and engineers and physical scientists to synthesise a wholly new approach to understanding biological functional behaviour in health and disease.

The transduction of chemical concentration into an electrical signal (usually a voltage), which can be recorded and interpreted, can be based on any of the fundamental properties of the molecules under investigation. One obvious characteristic is the interaction with electromagnetic radiation in the form of (i) infra red, which is characteristic of the bonds, and (ii) visible or ultraviolet light, characteristic of the molecular orbital energies. The advantages include a rigorous physical relationship between the absorption of radiation and the quantum mechanical properties of the molecule under investigation.

2.3 Molecular Recognition

Amperometric and voltammetric devices can select the analyte by applying an appropriate electrode potential. This can be further refined by using more advanced signal processing routines, also described below in Sect. 2.4.4. Similarly, recognition is intrinsic to the development of the membrane potential and the core technology employed in ion selective electrodes. This is typically achieved by ion exchange, neutral carriers or glassy materials. Molecular-level recognition for a dynamic device such as an amperometric sensor is not efficient if simply based on a "lock and key" mechanism. Some larger order change in the receptor molecule must be detected. This need not be in the molecular structure, though this helps, but could, for example, be a change in the free energy relationships as exploited in ion selective electrodes. All intermolecular forces can be important in recognition ranging, in order of increasing magnitude, from London dispersion/Van der Waals forces, dipole interactions, hydrogen bonding, ion-dipole interactions to electrostatic attraction. The range and distance dependence of these forces varies greatly. Ideally, these interactions should be rapid and reversible to reduce the impact of history on the sensor. If the receptor entity changes its structure as a result of binding the target, this can be detected by, for instance, surface plasmon resonance, changes in ion current through a nanopore and changes in capacitance or conductance. Alternatively, the recognition element can catalyse a reaction whose products can be detected by a chemical sensor.

As the number of potential targets increases, selectivity becomes more challenging and engineering the interface between the sensor and the tissue or solution sample becomes essential. There is a range of strategies that can be adopted. Historically the first of these was to use enzymes. Millions of years of evolution have led to exquisite selectivity, for example the first enzyme to be exploited in a biosensor, glucose oxidase from *Aspergillus niger* only catalyses the reaction of oxygen with the β-anomer of the D isomer of glucose. However, most enzymes are more promiscuous and certainly less stable, factors which have led to undue optimism in the early stages of biosensor development. Methods for engineering selectivity at the interface are summarized below:

Gas Selective Membranes – If the target analyte is a neutral molecule and the interferent is ionic, then interposing a gas permeable membrane such as PTFE (Teflon) between the test solution and the sensor will prevent the ionic species reaching the working electrode. The condition for this is that the effective pore size must be below two diameters of a water molecule. Ions can go nowhere without their accompanying water molecules that solvate them. A complication with this strategy is that the counter and reference electrode must also be behind the membrane since ions are also the charge carriers between the counter and working electrodes. This principle was first reduced to practice by Leland Clark for what is now universally known as the Clark O_2 electrode. The Clark electrode has been the method of choice for determining blood oxygenation since the late 1950s.

Selective Binding and Catalysis – Should the target analyte be oxidised or reduced at a similar potential to an interfering species, exploiting some selective chemistry of the target species can sometimes be successful. A typical example of this is the nitric oxide sensor first reported by Malinski [13] who used a Ni(II) (porphyrin) modified electrode surface to reduce the operating potential for oxidation of NO.

Amperometric Enzyme Electrodes – The key idea is to exploit the extraordinary selectivity of enzymes, which evolved over millions of years of natural selection. In these systems, there is no direct oxidation of the target analyte by the electrode. The analyte reacts catalytically with the enzyme to produce a reaction product which is then detected. The so-called "first generation" biosensors operate on this basis, the first reported example of which for the determination of glucose was published by Updike and Hicks in 1967 [14]. This approach was commercialised successfully by Yellow Springs Instruments. The underlying chemistry is shown below:

$$Glucose + O_2 \rightarrow Gluconolactone + H_2O_2 \tag{2.2}$$

The enzyme glucose oxidase (GOD) present, initially with its co-factor flavin adenine dinucleotide (FAD) in its oxidised form, is reduced in the process to GOD/$FADH_2$. Re-oxidation of the enzyme in nature is achieved by oxidation by dissolved O_2 which in turn is reduced to hydrogen peroxide. The hydrogen peroxide (H_2O_2) is detected by oxidation on a platinum electrode held at +0.65 V. The enzyme (or rather its cofactor) is reduced in the process and needs to be re-oxidised. The enzyme is immobilised by cross-linking with glutaraldehyde or by an electropolymerised film [15] or even by simple adsorption. An even simpler strategy can be employed where the working electrode is made of a conducting composite material. With the addition of suitable stabilisers such as polyethlyeneimine or dithiothreitol, enzymes can be incorporated into the bulk of the conducting carbon-epoxy composite to provide a cheap, extrudable or printable biosensor [16]. There are several comprehensive reviews of enzyme immobilisation techniques [17]. An ingenious molecular level assembly has been described by Willner [18] where the flavin redox centre is first immobilised followed by spontaneous self-assembly of the apoenzyme onto its co-factor.

The major problem with the first generation biosensors is that there are several common interferents which are also oxidised at +0.65 V, notably uric acid, ascorbate and acetaminophen. An alternative strategy was adopted for the second generation biosensors where it was recognised that the oxygen in the above reaction is in fact regenerating the enzyme. This is shown schematically in Fig. 2.1.

In this figure, the electrode is on the right hand side of the diagram, the test solution on the left. Substrate diffuses from solution (Step 1) through a membrane (where employed) (Step 2) to be oxidised by the enzyme (Step 3). The enzyme must be reduced in this process and needs to be regenerated by oxidation in Step 4. The mediator is then regenerated, in turn, by oxidation at the electrode surface (Step 5). For a concentration sensor, Step 1 or Step 2 needs to be the rate determining step. This ensures that the slope of calibration is not affected if the enzyme denatures

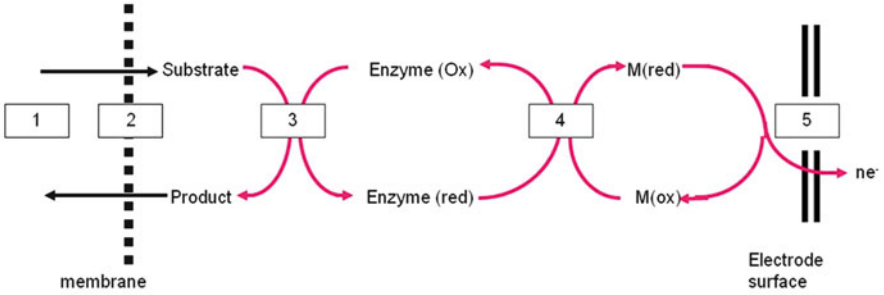

Fig. 2.1 A schematic of an enzyme-mediated electrode reaction showing the coupled mass transport and reaction steps. *1* Mass transport of the target analyte (which is also the enzyme substrate) in the bulk substrate. *2* Permeation through the membrane (if present). *3* Reaction of enzyme in its oxidised form with the substrate. *4* Regeneration of the oxidised enzyme by reaction with oxidised mediator. *5* Re-oxidation of the mediator at the electrode leading to current in the external circuit

slightly or loses activity. The mediator species can be chosen so that it undergoes fast reversible reaction kinetics at a potential where no other redox species are expected to react. Mediators which have been employed for this purpose include benzoquinone, the ferricyanide ion and various derivatives of the iron(II) compound ferrocene. The ethanolamine derivative of ferrocene is the mediator in the enormously commercially successful biosensor for glucose originally developed by Medisense, the ExacTech system. This concept was originally described by Cass et al. [19] using dimethyl ferrocene as a mediator. In this device, the enzyme was chemically immobilised on the surface of a screen printed carbon electrode. It would obviously be a lot simpler if the enzyme could be persuaded to react directly at the electrode surface. This cannot generally be achieved because the electron conduction path between the electrode surface and the redox centre of the enzyme is too great for there to be an appreciable tunnelling current. Third generation biosensors involve no directly added mediator species. There have been two broadly successful approaches – using electrodes made of low dimensional conducting charge transfer salts of tetracyanoquinodimethane (TCNQ) and redox wired enzymes. The former strategy was first described by Kulys and developed by Albery et al. – the most successful compound being the charge transfer salt of TCNQ and tetrathiafulvalene (TTF) (Fig. 2.2).

The mechanism was the subject of heated dispute for some time, it being believed that direct electron transfer was occurring. However, Bartlett was able to show that the TTF insinuates its way into the enzyme structure [20] to enable electronic conduction. A detailed mechanism for electrodes made from these materials has more recently been published by Lennox [21] showing that the mechanism is best understood as a form of heterogeneous mediation, where the mediator species is not soluble in water, but is soluble in the hydrophobic regions of the enzyme. Electrodes based on this technology have been used successfully for long-term studies of glucose metabolism in rats' brains over 10 days [22]. Wired enzymes tackle the problem more directly. Reactive sites in the protein structure are identified (or created by protein

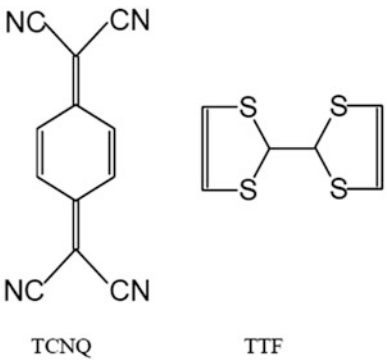

Fig. 2.2 Molecules involved in the classic 'third generation' biosensor

engineering) and reacted with redox active groups such as ferrocene derivatives, an approach now of some commercial significance and originally pioneered by Adam Heller's group [23]. This technology is now being applied with some success to power generation in biofuel cells by Heller [24].

Aptamers are a new class of molecules for recognition and binding based on oligomers of nucleotides, both RNA and DNA [25–27]. Typically 30–50 nucleotides long, they are developed by in vitro selection from libraries of random sequences in a process called SELEX: systematic evolution of ligands by exponential enrichment, first described in 1990 [28]. These binding entities have similarities to antibodies, but also notable advantages including thermal stability, ease of synthesis of appropriate sequences (using the polymerase chain reaction). They have a necessarily lower molecular weight than antibodies and can therefore be loaded onto surfaces (and sensors) at higher molar concentrations which, to some extent, can mitigate a lower binding constant (though extraordinarily high binding affinities can be and have been achieved [29]). Since aptamers are typically linear oligomers with well-defined end-group chemistry, conformation can be easily controlled and effective immobilisation is simpler than antibodies. Unlike antibodies, however, they recognize their targets by undergoing target induced conformational change. This conformational change lends itself naturally to FRET-type detection or fluorescent probe-quencher combinations, but can also be employed in electrochemical aptamer sensors (see Chap. 3) to take advantage of the very strong distance dependence of the tunneling probability in electron transfers. Several recent reviews cover the application of aptamers in biosensing [30–32] including their combination with nanotechnology [33].

Molecularly-imprinted polymers are a wholly synthetic approach. The essential idea is to prepare a polymer film with cavities that selectively accept the target molecule. These polymers are prepared from a monomer in the presence of the target, acting as a template, which is then washed out. The advantages are obvious: non-biological molecules are potentially more stable in storage and use than antibodies or enzymes; the methodology ought to be generalisable, versatile and cheap and the polymers can be prepared under sterile conditions and are likely to be more stable under common sterilisation conditions. Microbeads and nanofibres can

be prepared as well as films, giving rise to a reagent which can be produced in bulk and implemented in a sensor as needed. Applications to sensors in general [34, 35] and to electrochemical sensors in particular [36] have critically reviewed. Electrochemical approaches to polymerisation specifically for sensor applications represent a new approach and this has been reviewed recently [37].

Once molecular recognition has been achieved, the resulting change needs to be transduced into a signal that can be recorded, typically a voltage. Many different technologies have been employed in this role and the subject of recent reviews, for example: optical or photonic devices frequently based on optical fibres [38], thermistors and piezoelectric crystals either in shear mode (detecting mass changes) or using the surface acoustic waves. In addition to these well-established technologies, new sensing modes have arisen in recent years including nanoplasmonics [39]; field-effect organic transistors (ChemFET) [40]; microcantilevers based where target binding induces either a change in resonant frequency or a characteristic deflection [41], and most recently FET sensors based on grapheme [42]. Real world applications are thin on the ground whilst the biocompatibility and reproducible processing of such a new material is quantified. However, point-of care devices have been reported for prostate-specific antigen [43] and a flexible glucose sensor using CVD graphene has been produced [44]. The advantages of graphene are not yet apparent. The principal problem with all biomolecule-based devices remains the poor stability of the biomolecule itself. Therefore, these papers may be describing solutions to the wrong problem, unless the manufacturing process is greatly simplified and the cost of volume production in short order is addressed. The physiological milieu is an astonishingly hostile medium to work in and its heterogeneous structure, abundance of surface active and highly light absorbing structures has limited the range of applicable transduction modes to FETs, fibre-optic devices and electrochemical sensors.

FETs and fibre-optic devices have made substantial inroads in critical care sensing in recent years [45] (though the healthcare economics remains doubtful except for high value, high volume applications. Bedside optics cost upwards of $20,000, the probes themselves, which must be disposable cost >$300 each) but the dominant technology for implantable devices remains electrochemical and this is the subject of this chapter. A recent review of electrochemical biosensor technology can be found in [46].

2.4 Electrochemical Sensors

Electrochemical methods, electrochemical transduction and electroanalysis offer many advantages for biological measurement. The underlying physical description of electrochemical phenomena are beyond the scope of this chapter, but many excellent introductory [47] or more comprehensive texts [48–50] exist.

2.4.1 Potentiometry

Potentiometry is the electroanalytical technique where an electrode potential or membrane potential relative to a suitable reference electrode can be related to the analyte concentration, or strictly its thermodynamic activity. Potentiometric devices have the following characteristics:

- The system is at equilibrium; no current is passed and the analyte is not consumed;
- Instrumentation is simple, all that is required is a reference electrode and a high impedance voltmeter;
- Selectivity is inherent. The selective element is typically an ion selective membrane or a metal oxide coating;
- The response is logarithmic. Typically, there is a 59 mV change in output per decade change in concentration. This leads to a large linear dynamic range but leads to poor sensitivity in electromagnetically noisy environments.
- The practical dynamic range is hard to define since it is determined by deviations from the log-linear response at both ends of the calibration working curve.

The majority of potentiometric devices are based on the exploitation of equilibrium potentials at selective membranes. Such devices that have found to have broad applicability characteristics are, in many cases, commercially available, e.g. the glass pH electrode and microelectrodes have been used in biological media for decades and several tutorial and introductory books and chapters have been published [51–54].

2.4.1.1 Underlying Principles of Operation

Classically, potentiometry considers reduction-oxidation (redox) equilibria of the following kind:

$$M^{n+} + ne^- \rightleftharpoons M \tag{2.3}$$

Such redox reactions, usually coupled with a solubility equilibrium between the metal ion M^{n+} and some anion, e.g., Cl^- usually only find analytical use as reference electrodes (*vide infra*).

However, most analytically useful devices are based on membrane equilibria and are known as ion selective electrodes, ISEs. These have their origin in the glass pH electrode, found in thousands of general chemistry, biology and pathology labs worldwide since its original description by Cremer in 1906 [55].

The most commonly used ion selective membranes are glass and crystalline solids (for example europium (III) – doped LaF_3 for fluoride selective electrodes) that are supported liquid ion exchangers or ionophores (ion-binding molecules) dissolved in polymers with suitable plasticisers.

Regardless of their physical embodiment, all ion selective electrodes are based on thermodynamic equilibrium across an ion selective membrane. Understanding of the underlying phenomenon is essential if real devices are to be operated successfully. The starting point is that the free energy of all species in all phases must be the same throughout the system for the system to be at equilibrium. The key parameter for ions, which bear an electrical charge, is their *electrochemical potential* $\overline{\mu}$, which is the sum of the partial molar free energy, i.e. the chemical potential μ and the electrical potential ϕ appropriately scaled from electrician's units (volts) to chemist's units (joules per mole) using Faraday's constant, F the charge in coulomb on one mole of electrons.

$$\overline{\mu}_i = \mu_i + zF\phi \tag{2.4}$$

where z is the formal charge on ion i. If we have two solutions α and β separated by an ion selective membrane, the equilibrium condition is:

$$\overline{\mu}_{i(\alpha)} = \overline{\mu}_{i(\beta)} \tag{2.5}$$

Expansion of the electrochemical potential terms leads to:

$$\mu^{\circ}{}_{i(\alpha)} + RTlna_{i(\alpha)} + zF\phi_\alpha = \mu^{\circ}{}_{i(\alpha)} + RTlna_{i(\alpha)} + zF\phi_\alpha \tag{2.6}$$

where subscripts α and β refer to the two solution phases α and β. a_i is the activity of ion i which can be approximated for infinitesimal concentrations to the concentration of the ion. Rearrangement gives an expression for the membrane potential, ϕ_m, the electrical potential difference between phases α and β arising from different ionic activities:

$$\phi_m = \phi_\alpha - \phi_\beta = \frac{RT}{zF} ln\left(\frac{a_{i(\alpha)}}{a_{i(\beta)}}\right) \tag{2.7}$$

Provided therefore that we control the ionic activity on one side of the membrane, the membrane potential relative to a suitable reference electrode will depend only on the ionic activity of the ion in the outside solution. At this stage, it is worth pointing out that the membrane potential will only *free ion concentration* not total ion concentration. This is a unique selling point of this technology and ensures that ISEs will continue to be used, as the ratio of free: total ionic concentration continues to be of interest and biological relevance.

Implementation of a practical device exploiting this phenomenon therefore simply requires (i) reference electrodes to sense the solution potential (ii) a selective membrane and (iii) a high impedance voltmeter. This is shown schematically in Fig. 2.3.

The *reference electrodes* are designed such that the galvani potential difference *between* the terminal connection at the top of the electrode and the solution is essentially independent of the composition of the solution. By far the most widely

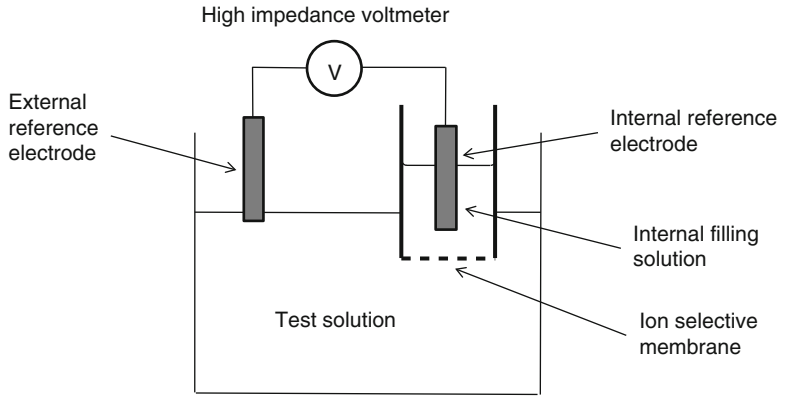

Fig. 2.3 Schematic of an ion selective electrode set-up

used reference electrode in both potentiometry and in amperometry is the silver|silver chloride electrode. This important electrode is based on the following equilibrium:

$$AgCl(s) + e^- \rightleftharpoons Ag(s) + Cl^- \tag{2.8}$$

At equilibrium, the electrochemical potentials of the reactants and products must be equal:

$$\overline{\mu}_{AgCl} + \overline{\mu}_{e^-} = \overline{\mu}_{Ag} + \overline{\mu}_{Cl^-} \tag{2.9}$$

$$\therefore \mu_{AgCl} + (\mu_{e^-} - F\emptyset_M) = \mu_{Ag} + (\mu_{Cl^-} - F\emptyset_s) \tag{2.10}$$

The chemical potential of the chloride ion is given by:

$$\mu_{Cl^-} = \mu^\circ{}_{Cl^-} + RTln([Cl^-]) \tag{2.11}$$

where $[Cl^-]$ is the concentration (strictly activity) of the chloride ion. For pure solids AgCl and Ag, the chemical potentials are equal to their standard chemical potentials. This means that the potential difference between the metal and the solution is given by:

$$\emptyset_M - \emptyset_S = \frac{\Delta\mu^\circ}{F} + \frac{RT}{F} ln\left(\frac{1}{[Cl^-]}\right) \tag{2.12}$$

where $\Delta\mu^\circ$ is a lumped constant of the standard chemical potentials of the silver metal, chloride ion, electron and silver chloride solid. The key consequence of this equation is that, provided that we keep the chloride ion concentration constant, the potential difference between the metal and the solution for this electrode will be constant. This is achieved in practice by placing a chloridised silver wire in a

solution of potassium chloride of a known concentration inside a small glass or plastic tube. Electrical connection to our test solution or internal filling solution is via ionic contact through a fritted glass disc made of either Vycor or a porous polymer that allows ion transport but prevents bulk fluid flow. Therefore, if, as in Fig. 2.3 above, we place a silver-silver chloride electrode either side of the membrane, any change in the measured potential must be due to changes in the membrane potential.

Reference electrodes remain more of a problem for biological application than is generally acknowledged in the literature. Screen-printed Ag | AgCl is cheap enough to be considered disposable and is a scalable technology [56]. Idegami et al. were able to incorporate electrolyte in a sodium alginate paste in the screen-printing process to produce the complete device. Alternative materials have been explored and amongst the most promising are using silver tetramethylbis (benzimidazolium) diiodide [57] and nanoporous platinum solid state layer-by-layer polyelectrolyte junction that have been reported for lab-chip applications and show great promise [58].

The experimental set-up sketched out above will give an idealised logarithmic response to changes in thermodynamic activity that can be represented as:

$$E = E^{\circ} + \frac{RT}{zF} lna_i \tag{2.13}$$

where a_i is the thermodynamic ion activity. This can, under suitable circumstances, be approximated to concentration but it should always be remembered that the underlying response is to activity, not concentration, and that this places constraints on the experimenter.

2.4.1.2 Calibration

The preparation of activity standards is not usually an option for biomedical application of ion selective electrodes. Activity depends strongly on the chemical composition of the sample matrix, especially the ionic strength, I.

$$I = \frac{1}{2}\sum_i c_i z_i^2 \tag{2.14}$$

where c_i is the concentration o ion I and z_i is the absolute charge, including the sign. The relationship between activity and concentration is given by:

$$a_i = \gamma_i c_i \tag{2.15}$$

where γ_i is the ion activity coefficient, essentially a fudge factor that corrects for the non-ideal behaviour of solutes at real concentrations. As the concentration approaches zero, ideal behaviour is better approximated and the ion activity

Table 2.1 Examples of the divergence of activity from concentration for physiologically important ionic species

Concentration/mol dm^{-3}	γ (K^+)	γ (Ca^{2+})	γ (Cl^-)
0.01	0.903	0.675	0.903
0.05	0.820	0.485	0.805
0.1	0.774	0.269	0.741
0.2	0.727	0.224	0.653

coefficient tends to unity. Concentration deviates from activity to a greater extent the greater the ionic strength. Approximate values of $\gamma_{\pm}$, the mean activity coefficient, can be estimated from the ionic strength using the Debye-Hückel theory. For low (sub-millimolar) concentrations, the following relationship can be applied:

$$log_{10}\gamma_{\pm} = -A|z^{+}z^{-}|\sqrt{I} \tag{2.16}$$

where z^+ and z^- are the charges on the cation and anion respectively. Higher concentrations require the use of the Debye-Hückel extended law. However, for real analytical situations, matrix composition cannot usually be determined. Large and potentially important deviations from unity occur at relatively low ionic strengths. Table 2.1 shows the potential extent of this problem for common ions.

The ionic strength of typical biomedical specimens is around 0.2 mol dm^{-3}. Failure to take variations in ionic activity into account can lead to serious errors. This can be true for apparently well-established measurement such as the determination of pH; the ion activity coefficient for H^+ at 37 °C and the physiological ionic strength around 0.83 [59].

So how can selective membrane potentials (at the heart of both ISEs and ion selective field effect transistors) be exploited to determine chemical concentrations? The key is to ensure that calibration solutions have the same ionic strength as the unknown sample. This is relatively easy to achieve for physiological fluids where the ionic and protein compositions are known from decades of measurements over millions of patients. Combining Eqs. 2.13 and 2.15 above yields:

$$E = E^{\circ} + \frac{RT}{zF} lnc_i + \frac{RT}{zF} ln\gamma_i \tag{2.17}$$

so it can be seen that, provided the ionic strength is kept constant, then the measured cell potential can be related to the concentration. This can be achieved in the chemical pathology or clinical biochemistry lab by preparing concentration standards (i.e. solutions of known concentration used to prepare calibration working curves) in *total ionic strength adjustment buffer* (TISAB). This will have a much higher ionic strength than the analyte and usually contain a pH buffer too. Provided that I (TISAB) $>> I$ (analyte) and that the analyte is also diluted with TISAB, the cell potential can be approximated as:

$$E_{cell} = K + \frac{RT}{zF} lnc_i \tag{2.18}$$

where K is a constant that now includes the activity coefficient. For historical reasons, the response of an ISE is usually reported in base 10 logarithm as:

$$E_{cell} = K + \frac{2.303RT}{zF} log_{10} c_i \tag{2.19}$$

At 25 °C this means that the measured cell potential changes by 59 mV per tenfold change in concentration for a singly-charged analyte.

Typically 6–10 calibration standards are prepared, most accurately achieved by dilution with TISAB from a freshly prepared stock solution. The concentration range should bracket the expected concentration range of the unknown samples and be centred on the expected mean value, to minimise confidence limits from the linear least squares fit.

As always with analytical measurement, some quality control is always required. This can involve the "blind" analysis of *certified reference materials* (CRM) where available. Alternatives to the use of CRMs include analysis of one or more samples using a method dependent on a different physical principle or use of standard additions.

The method of standard additions is an important alternative to the use of calibration working curves, especially for ion selective electrodes. In complex or poorly-characterised media, it may not be possible to measure the concentration of, and characterise the response, to all potential interferents. In addition, ISE performance may be impaired by "spectator species" such as plasma proteins. In this method, the analyte sample is added to TISAB and the ISE potential is measured. An aliquot of standard solution, also prepared in TISAB is then added to the prepared sample and the new potential is recorded. Equation 2.18 is then employed. Two potentials and two unknowns enable calculation of the initial concentration in the prepared analyte, enabling calculation of the concentration in the original specimen.

The use of TISAB effectively deals with the thermodynamic response of the ISE membrane. For in vivo or in situ use however there are no easy fixes. Frequently, it may be reasonable to infer a quantitative or semi-quantitative *change* in concentration from an implanted ISE response, but care must be taken to avoid over-interpretation of experimental data.

The logarithmic response of ISEs has important consequences. The dynamic range of ISEs is typically very large and a six order of magnitude range is not unusual. This can be an advantage for environmental analysis where large dynamic ranges are expected. However, for many biomedical analytes, concentrations are highly controlled. The logarithmic response is therefore a big disadvantage since ion selective membranes have impedances that are >10 MΩ. Electrochemical devices are non-linear and have rectifying properties and so the electromagnetically-noisy environment encountered in the healthcare setting can lead to large errors. This can be minimised by careful design, as recently reported for intracellular Ca^{2+} and H^+ microelectrodes using concentric micropipettes to reduce the impedance and give improve response times, around 15 and 5 ms for H^+ and Ca^+ respectively [60] though, as the authors acknowledge, this was inspired by earlier work [61].

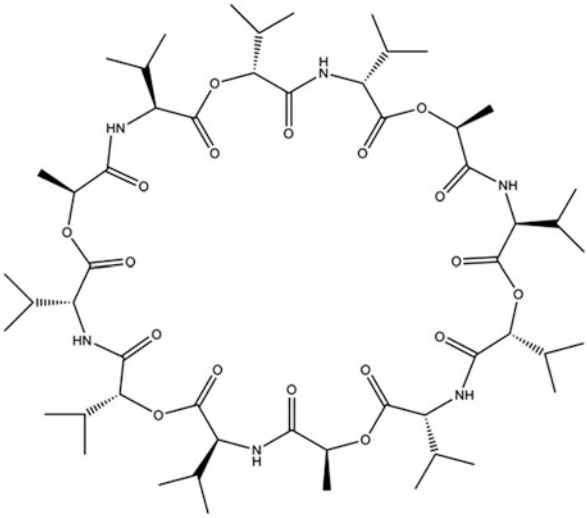

Fig. 2.4 Valinomycin, a bacterially-derived antibiotic and ionophore of choice for K^+ sensors

2.4.1.3 Selectivity

Selectivity of the carrier molecules varies greatly. A quantitative assessment is essential for ascertaining fitness for purpose. Commercially-available ionophores and ISEs usually report selectivity coefficients for single potential interferents. These are defined in a modified version of Eq. 2.19, known as the Nickolsky-Eisenman equation:

$$E = K \pm \frac{2.303RT}{F} log_{10}\left(c_i^{1/z_i} + \sum k_{ij} c_j^{1/z_j}\right) \tag{2.20}$$

where k_{ij} is the *selectivity coefficient* for interfering ion j over the analyte ion i. z_i and z_j are the charges on the analyte and interferent respectively. The key assumption is that there are no synergistic effects between interferents. This is more likely to be true for low concentrations of both analyte and interferent, i.e. there is an adequate concentration of unbound ionophore.

For example, the potassium ion ionophore, valinomycin (Fig. 2.4), when used in a PVC membrane plasticised with dioctyl adipate, has a selectivity coefficient for potassium ions over sodium ions of 6.2×10^{-6}. We can calculate the maximum expected error when this ISE is used to measure potassium ions in plasma. The normal range of potassium ion concentration in plasma is 3.2–5.1 mmol dm^{-3}. The normal range for sodium ions is 135–146 mmol dm^{-3}. The maximum expected error is calculated by substitution into Eq. 2.5:

$$\begin{aligned} \%error &= \frac{k_{K^+Na^+}.c_{Na^+}}{c_{K^+}}.100\% = \frac{6.2 \times 10^{-6} \times 146 \times 10^{-3}}{3.2 \times 10^{-3}} \times 100\% \\ &= 0.028\% \end{aligned} \tag{2.21}$$

The final point to make about selectivity is that a properly functioning ISE will always give a potential whether or not the target analyte is present. This rarely

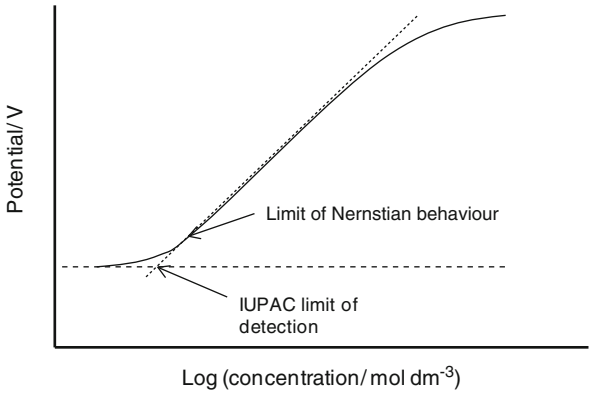

Fig. 2.5 Schematic showing the IUPAC limit of detection for an ISE

presents an issue in biomedical measurement where the concentration of the analyte is unknown but it is known to exist. However, if this is not the case, independent confirmation of the analyte's presence is required using, for example, atomic spectroscopy.

2.4.1.4 Limit of Detection

A further consideration in the use of ISEs is the limit of detection (LOD). For most analytical devices, this is defined as the smallest signal statistically different from the background noise. The logarithmic response of an ISE means that zero concentration is not defined. A different approach is therefore adopted. The log-linear range of the ISE is extrapolated to where it intersects the line describing the zero response. This is the IUPAC agreed definition of LOD of an ISE and is shown schematically in Fig. 2.5.

2.4.1.5 Other Potentiometric Devices

Whilst ISEs (and the related ISFETs) dominate the potentiometric sensor, an important class of potentiometric device for biomedical application is the metal-metal oxide electrode used to measure pH. Glass pH electrodes suffer from obvious disadvantages in the in vivo application: extreme fragility, potential hazard on failure, high electrical impedance and high skill level for manufacturing, all of which militate against commercial, or even research availability. A suitable alternative is the metal-metal oxide electrode which exploits the equilibrium between a hydrated metal oxide and its hydroxide. The advantages of such devices were recognized early and are the subject of a review by Ives [62]. More recent reviews have been published by Głab [63] and O'Hare [64]. The underlying phenomenon exploited in metal-metal oxide electrodes is the measured electrode potential due to the equilibrium between a sparingly soluble salt and its saturated solution, i.e. the

potential depends on the thermodynamic solubility product of the oxide. MMO electrodes are a special case of this kind of electrode since the anion (OH^-) participates in the self-ionisation of the solvent and the equilibrium between unionized water, protons and hydroxide ions. This gives rise to a potential dependence on pH which should therefore be given by:

$$E = E^{\circ}_{M,MO,H^+} - \frac{2.303RT}{F} pH \tag{2.22}$$

where R, T and F have their usual meanings. The standard potential term includes the standard potentials for all the participating species, the solubility product of the metal oxide and the ionisation product of water.

The ideal properties of a MMO electrode have been listed by Ives as:

- The metal must be sufficiently noble as to resist corrosion;
- It must be possible to obtain the metal in a reproducible state;
- The oxide must be stable. (This is incompatible with (1), though in practice, the oxide must only be scarcely soluble);
- It must be possible to obtain the oxide in a reproducible state;
- The oxide must be scarcely soluble yet able to participate in the equilibrium reaction sufficiently rapidly to give an adequate current density.

These properties, though scarcely achievable practically (1 and 5 are strictly contradictory) are useful guides to experimentation.

No MMO system has been found which is well-behaved for all applications, though antimony electrodes have been widely used for many years in medical application, an early example being a 1941 account of continuous recording of the pH of human gastric contents [65]. Relative ease of fabrication using antimony shot melted into a pulled glass capillary has led to application as potentiometric sensing tips in scanning electrochemical microscopy [66]. However, there are several serious drawbacks to using antimony electrodes in vivo: Ives has noted that they must be used in aerated solutions and that Nernstian or even rectilinear responses cannot be relied upon. The solution must not contain oxidising, reducing agents or complexing agents such as citrate, oxalate, tartrate or certain amino acids. There is a response to dissolved oxygen which is caused by localised corrosion for which the cathode reaction is reduction that inevitably leads to sensitivity to stirring.

As a consequence of the shortcomings of the two most widely used pH sensors (glass membrane ISE and the antimony electrode), there has been a substantial recent interest in pH sensors based on hydrated iridium oxide. These devices are of interest due to their reported stability in a wide range of aqueous solutions, low impedance, fast response times and the compatibility of iridium with C-MOS processes allowing the prospect of integrated devices. There has consequently been considerable activity around iridium oxide sensors in recent years. Some aspects of biological applications have been reviewed by O'Hare [64]. This is a genuinely robust piece of technology and, in conjunction with a boron-doped

diamond sensor for histamine (*vide infra*) has been used to elucidate the control pathways for acid production in the stomach of an isolated perfused guinea pig stomach in single sensor measurements [67] and in an array format [68].

There are several methods for preparing these devices: electrochemically generated iridium oxide films (widely known as AIROF – anodic iridium oxide film) [69]; thermally generated iridium oxide (preparative methods are critically compared by Głab [63]); direct electrodeposited iridium oxide from the oxalate complex, developed by Yamanaka [70], and iridium oxide can also be deposited directly using RF sputtering. Thermally deposited and AIROF electrodes appear to be chemically distinct. Iridium oxide deposited using the Yamanaka method has current–voltage characteristics closer to thermally generated iridium oxide. The most convenient method in most applications is that described by Yamanaka, direct electrodeposition by electrolysis of the oxalate complex from alkaline solution:

$$\left[\left[Ir(COO)_2(OH)_4\right]^{2-}\right](aq) + 2OH^- \rightarrow \left[IrO_2(OH)_2.2H_2O\right](s) + 2CO_2 + 2e^- \tag{2.23}$$

where the oxalate ligand is oxidised to CO_2 at the electrode substrate leaving a compact deposit of hydrated iridium oxide on the substrate. Recent work on IrOx devices has coalesced around this method as it is a reliable technique for generating reproducible microsensors, despite its origins, as in electrochromic displays and reliable devices that have been produced in the 3–10 μm range [71]. An improved, faster method based on essentially the same reaction has been reported [72] for the deposition on acid-etched titanium substrate, which show great potential for application in integrated sensing devices, since the usual substrates (gold or platinum) are less compatible with many microfabrication facilities.

Reliable protocols for the three most common methods are given below:

- ***Electrolytic Preparation of AIROF Electrodes*** – Iridium is a dense, brittle and expensive metal, to the extent that it is frequently more convenient to work with small pieces of iridium wire connected to platinum or cheaper material. Iridium wire (0.125 mm diameter, 4–5 mm in length, 99.99+%) was butt-welded to platinum wire in a natural gas/O_2 flame. Spot welding is similarly successful but silver-loaded epoxy shows a high fail rate. The wire needs to be insulated everywhere but the sensing surface. This can be accomplished by dip coating in Epoxylite resin. Additional mechanical strength can be achieved by embedding in a hypodermic needle using low viscosity epoxy resin. Electrode tips were prepared by sawing on the bevel using a low speed saw (Buehler) followed by polishing on emery paper (1,200 grit and 2,500 grit) and aqueous alumina slurry (6 μm, 1 μm and 0.05 μm, Buehler) on polishing cloths with ultrasonic cleaning in water between grades. The oxide film was generated by cycling the potential in sulphuric acid (0.5 mol dm^{-3}) at 2 V s^{-1} for 8,000–12,000 cycles between the potentials of hydrogen and oxygen generation finishing with a 10 mV s^{-1} stopping at the main anodic peak. An iridium rod and Ag | AgCl | 3 M KCl

served as counter and reference electrode respectively. The reference electrode was connected to the cell using a K_2SO_4 (0.3 mol dm^{-3}) salt bridge to minimise chloride ion infiltration. This has been found by present authors and others to be critical in the preparation of stable films. Cyclic voltammograms were recorded at various intervals to assess the extent of oxide film growth. In all cases, the resulting AIROF electrodes were soaked for 48 h in deionised water (>15 MΩ cm) prior to use. For additional stability in biological measurement, we have found that Nafion coating is very successful and barely affects sensitivity or response time. Nafion films were applied and annealed at 120 °C according to the protocol described by Harrison and Moussy [73]. Calibration from pH 3 to 12.1 gave a super-Nernstian response of (69 ± 2) mV per pH unit. Comparison of calibration curves recorded in nitrogen and oxygen-sparged solutions revealed a maximum perturbation of 0.9 mV at pH 7.4. This places an absolute limit on the accuracy of 0.0125 pH units if the oxygen concentration is unknown, though this does of course represent the worst-case scenario.

- ***Thermally Prepared Iridium Oxide Electrodes –*** Iridium wire was annealed in a natural gas flame, straightened and carefully cleaned by sonication in acetone followed by rinsing with deionised water. After drying, one end (approx. 2 mm) was wetted with NaOH solution (1 mol dm^{-3}) and the wire was heated to 800 °C in a muffle furnace for 30 min. This was repeated until a blue-black coating was clearly visible to the naked eye. This typically took five to six applications. The electrode was soaked for 3 days in deionised water before use. All but the electrode tip (approximately 0.5 mm) was insulated using FEP/PTFE dual shrink tubing (Zeuss). Nafion films were applied using the technique described above. Calibration in Britton-Robinson buffer over the physiologically-relevant pH range of 6.5–8 gave a slope of 59.5 mV/pH (r = 0.9999).
- ***Direct Anodic Deposition of Iridium Oxide on Gold*** [67] – Initially, a 75-μm gold wire insulated in Teflon (overall diameter 140 μm, A-M Systems Inc.) was threaded through a 27-gauge hypodermic needle. A copper or silver wire was attached to the gold wire with silver epoxy resin to form an electrical contact. Epoxy resin (Robnor Resins, CY1301 and HY1300) was used to fill the internal volume of the needle and left for 2 days to cure according to the manufacturer's instructions. The lower end of the needle was cut perpendicularly using a diamond saw (Buehler) to expose the 75-μm Au disk microelectrode. Successive polishing with aqueous slurries of 1-, 0.3-, and 0.05-μm alumina in deionized water with rinsing and sonication at each polishing stage was necessary to ensure a flat electrode surface. Cyclic voltammetry (CV) in 0.5 M H_2SO_4 was used to electrochemically clean the gold electrode surface prior to deposition. Using the same technique, the transport-limited currents were recorded in 1–10 mM $Ru(NH_3)_6^{3+}$ in supporting electrolyte to assess the surface of the gold electrodes. When the recorded limiting current had reached the theoretical value for a 75 μm diameter microelectrode in a known concentration of analyte, the electrode was considered ready for use. Anodic electrodeposition of the iridium oxide film onto gold microelectrodes was performed using a deposition solution described by Yamanaka [70]. Briefly, 0.15 g of iridium tetrachloride, 1 mL of 30 % w/w

H_2O_2, and 0.5 g of oxalic acid dihydrate were added gradually in a 100 mL of water at 0.5 h intervals and left to dissolve in a stirred solution. Anhydrous potassium carbonate was then added gradually to the solution until the pH reached ≈10.5 forming a pale yellow solution. The solution was then covered and left at room temperature for 48 h to stabilise until a colour change to pale blue was achieved. This blue solution was stored in the refrigerator and could be used for a few months to successfully produce IrOx films.

The anodic electrodeposition of the IrOx films on gold microelectrodes was achieved amperometrically using a constant potential method. A potential between 0.6 and 0.7 V versus a double junction reference electrode (DJRE) was applied for several minutes to produce a thin, uniform, and defect-free film. The DJRE with a calomel inner junction reference system was used with a sodium sulphate (0.1 M) outer junction solution to prevent chloride ion permeation [64]. Assuming 100 % faradic efficiency of electrodeposition, the total amount of iridium oxide was calculated to be 0.006 μg when the deposition potential, Ed, of 0.65 V was applied for 2 min (current density 0.83 mA cm^{-2}). The coated microelectrodes were washed and placed in deionized water for at least 2 days prior to use to allow redistribution of ions and hydration to occur and a stable open circuit potential to develop. In our lab, once this initial hydration had occurred, the electrodes could be rinsed in de-ionised water and stored dry for months. Re-use only required hydration for a few minutes. Composition and integrity of the film can be tested at regular intervals by examining the cyclic voltammogram in 0.1 mol dm^{-3} H_2SO_4.

Typical performance is shown in Fig. 2.6 (taken from [67]).

2.4.1.6 Recent Developments in Ion Selective Electrodes

For nearly 100 years, research in ion-selective electrodes was largely incremental and focused on improvements in selectivity, novel ion carriers and applications away from the laboratory including point-of-care and environmental applications. This mature technology, which is relevant to biomedical applications, is reviewed in two excellent papers by Pretsch, one of the most significant players in this field [74, 75]. However, there have been significant developments in the last 10 years in both theory and practice which have led to the so called “new wave” ISEs. These significant developments have been the subject of two recent reviews [76, 77].

The conventional theoretical analysis, the classical total equilibrium model essentially followed above, is, of course, a gross simplification of the actual disposition of the ions, carriers and electric fields present in real devices. However, this essential, and deliberate, simplification is entirely adequate to the task of supporting the user of sensor technology. However, more sophisticated analysis is required to account for the variable and time-dependent responses of ISEs in long-term and to provide insight that have since led to improved performance. These theoretical advances are described by Lewenstam [78].

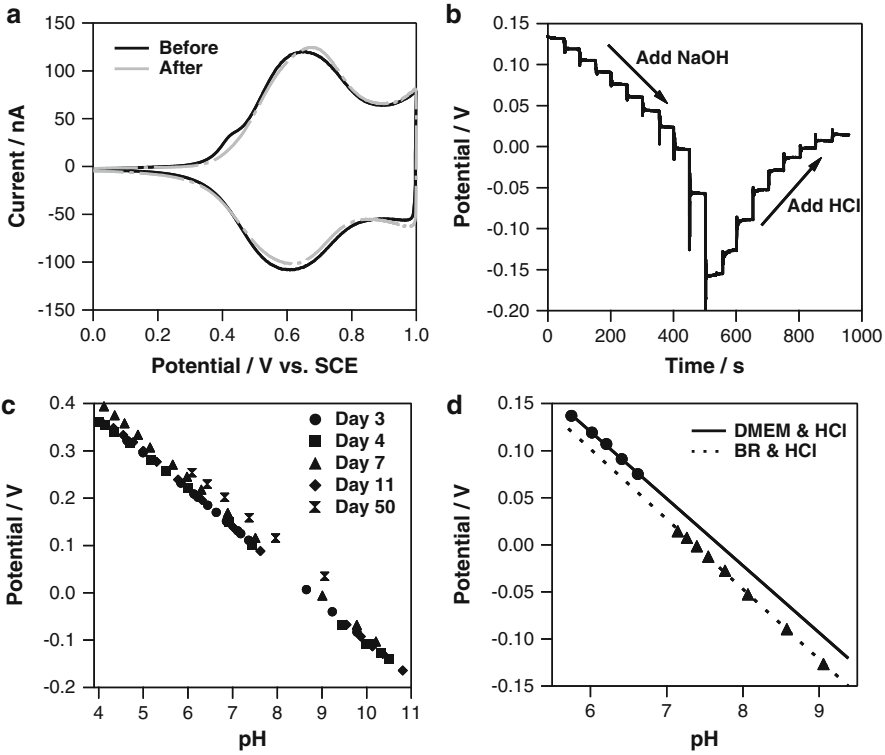

Fig. 2.6 Typical responses of a 75 μm diameter gold microelectrode coated with iridium oxide. (**a**) shows the cyclic voltammetric response in 0.5 M H_2SO_4 before and after exposure to perfused stomach. (**b**) shows the electrode's open-circuit potential response to changes in pH during acid–base titration. (**c**) Typical calibration plots over 50 days showing excellent stability. (**d**) Calibration in Britton-Robinson buffer compared with calibration in tissue culture medium (DMEM) over the physiologically relevant range (Taken from Ref. [67])

The major change in ISEs however is the spectacular improvement in the limits of detection achieved in recent years, such that ISEs are now competitive with atomic spectroscopy. The initial insight was that whilst conventional ISEs had limits of detection around 10^{-6} mol dm^{-3} but picomolar LODs were obtainable with optical sensors using the same ionophores and essentially the same membrane technology (though with a vastly more expensive instrumentation). This led to the hypothesis that primary ions leaching from the membrane determine the LOD. By the simple expedient of incorporating an ion buffer into the internal electrolyte, Pretsch and colleagues were able to extend the limit of detection for a Pb^{2+} ISE from 4×10^{-6} mol dm^{-3} to 5×10^{-12} mol dm^{-3}.

New technology or the application of mature technology from other fields is being brought to bear on ISEs. Solid contact potentiometric sensors remain promising technology and their application to medicine and biology has been touted as early as 2000 [79]. Conventional microfabrication dielectrics have been found to be

suitable for both ISFETs and ISEs [80] and silicon nitride substrate have been used to make miniaturised Na^+ selective electrodes [81]. Solid-state devices have been reported for K^+ and Ca^{2+} based on electropolymerisation of polystyrenesulfonate-doped PEDOT on recessed gold discs insulated with glass, which are then covered with ion selective membranes [82]. Microfabricated devices have found application in cell culture where 2 μm or 6 μm ion selective devices for potassium ions and ammonium were formed in micropipettes microfabricated at the bottom of cell culture wells [83].

Screen printing is also an attractive technology as it is both cheap and widely available and has relatively low start-up and scale up costs. These are important factors which can otherwise restrict the development of new sensors to research-only or high value applications. Getting the reference electrodes to work without the current craft-intensive processes is essential for both ISEs and ISFETs and screen printed miniature solid state devices have been reported [84, 85] including a solid state screen-printed K^+ selective electrode [86].

Kapton-based K^+ and pH flexible microelectrode ISE arrays have been described by Buck [87, 88] and have been used to record on a beating heart during ischaemia. More conventional microfabrication of an ISE chip, complete with built-in reference electrodes has been reported by Uhlig et al. [89]. Usefully, comparative performance data for different membrane polymers and formulations are described and the chip arrays were used in a flow-through format for measurement of K^+ and Ca^{2+} concentrations in urine, human serum and whole blood. The advantages of array sensing are discussed in more detail below. Similarly, Yoon et al. [90] built arrays of ISEs for blood electrolytes (K^+, Na^+. Ca^{2+}, H^+, Cl^-). Whilst technology for blood electrolytes in the clinical setting is mature technology and there is no market pull for improved performance (the major costs are staff salaries and reagents), the novel reference electrode performance using a polyurethane coated reference electrode is reported to be sufficiently stable to reduce the requirement for repeated standardisation between measurements that will simplify operation and improve throughput. Conventional microfabrication gives inherent scalability and potentially reduced costs but the requirement for extensive post-production processing and limited market pull probably explain poor uptake of this technology so far.

2.4.2 Amperometry and Voltammetry

Potentiometric methods are passive and the selectivity is inherent, that is to say, it is built in to the membrane in the case of ISEs. Amperometric and voltammetric methods however, involve applying a non-equilibrium electrical potential and measuring the resulting current or current–voltage relationship to obtain quantitative (in the case of amperometry) or qualitative information. At the core of this technology is the transfer of electrons between the Fermi level of a usually metal electrode and the molecular orbitals of the target analyte. Oxidation involves the loss of electrons from the highest occupied molecular orbital whereas reduction

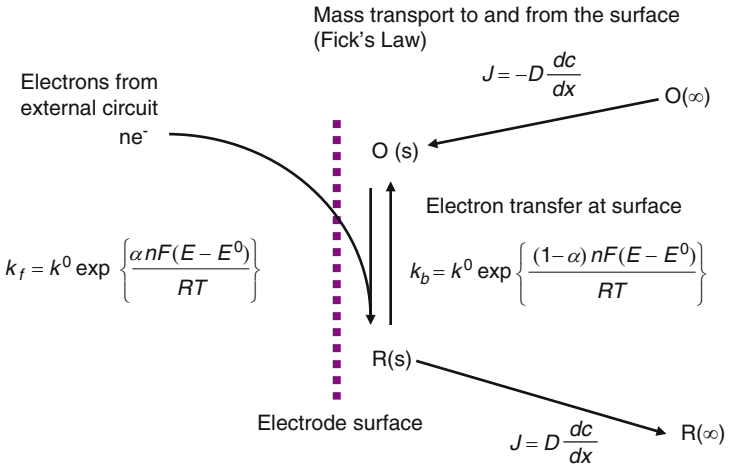

Fig. 2.7 A schematic of the simplest electrode reaction. The *dashed line* represents the electrode surface. The electrolyte solution is to the *right* of the electrode surface showing mass transport to and from the electrode surface (by Brownian motion). To the *left* of the electrode surface is the external circuit

involves electrons being injected into the lowest unoccupied molecular orbital. For some arbitrary pair of compounds where R represents the reduced form and O represents the oxidised form, the reaction can be written as:

$$O + ne^- \rightleftharpoons R \tag{2.24}$$

One or both of R and O can be solution free species or insoluble and bound to the electrode surface, or even be the elemental form of the electrode itself. The oxidation-reduction reaction shown above is the simplest scheme possible where only electron transfer is involved. However, for many real target analytes such as the monoamine neurotransmitters or dissolved gases such as oxygen or nitric oxide, the electron transfer is also associated with adsorption and proton transfers. In addition, there may in some cases also be changes of phase which further complicate an already intricate situation, but the core of an electrode reaction is the transfer of electrons between a molecule in an electrolyte solution and an electrode made of conducting or semiconducting material.

The electron transfer event is a very short range phenomenon; for aqueous systems the electron tunnelling event really only takes place over a few hundred picometres, about the same size as a hydrated metal ion (a hydrated K^+ ion has a radius of 330 pm). This short range has several important theoretical and practical consequences. Firstly, for a molecule to undergo a redox reaction is must be transported to within a bond length of the electrode surface. The simplest scheme describing an electrode reaction is shown in Fig. 2.7.

As can be seen for Fig. 2.7, the rate of mass transport to the surface must be equal to the rate of the electron transfer reaction at the electrode surface. The rate of

electron transfer, suitably scaled from chemists' units to electricians' units using Faraday's constant (*vide supra*) is given by the current through the external circuit. In one dimension (for the sake of clarity) this relationship is given by:

$$\frac{i}{nFA} = J = -D\frac{dc}{dx} \tag{2.25}$$

where F is Faraday's constant (96,485 C mol^{-1}), J is the flux (mol m^{-2} s^{-1}), D is the diffusion coefficient (m^2 s^{-1}) and dc/dx is the concentration gradient. Analytical expressions for the current at an electrode therefore essentially depend on being able to describe the concentration gradient for a specific electrode and boundary conditions. An excellent introduction to analytical and numerical approaches to these sorts of problems has been published by Compton & Banks [91].

The rates of the forward and backward reactions are given by:

$$Forward\ \ rate = k_f(c_O)_{x=0} \tag{2.26}$$

and

$$Backward\ \ rate = k_f(c_R)_{x=0} \tag{2.27}$$

The rate constant for the electron transfer depends exponentially on the applied potential. Whilst there are microscopic quantum mechanical descriptions, the empirical Butler-Volmer relationships with their familiar Boltzmann form are entirely adequate for most purposes:

$$k_b = k_b^{\circ} exp\left(\frac{\propto_A nFE}{RT}\right) \tag{2.28}$$

for the rate constant for the backward electrode reaction, and

$$k_f = k_f^{\circ} exp\left(\frac{-\alpha_c nFE}{RT}\right) \tag{2.29}$$

where n is the number of electrons transferred, R is the gas constant, T is the absolute temperature, E is the applied potential and k° is the standard heterogeneous rate constant. α_A and α_C are the anodic and cathodic transfer coefficients respectively. The can be related to the position of the maximum of the potential energy-reaction coordinate curve and Compton has recently demonstrated that the physical meaning may be associated with bond energies of the transition state. In any case, they sum to unity and typically have a value close to 0.5.

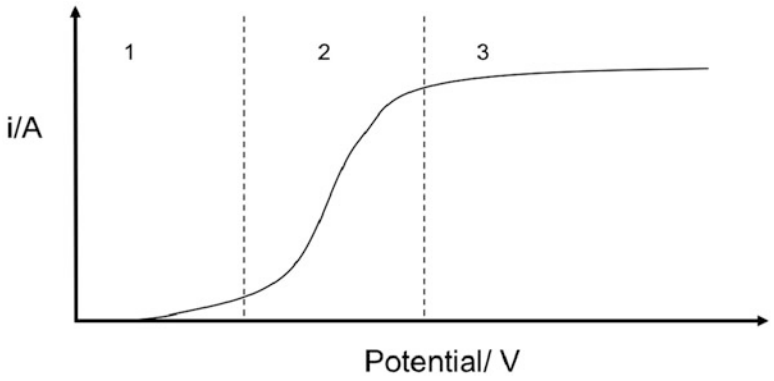

Fig. 2.8 A schematic representation of the current-voltage relationship

At the equilibrium potential, E_e given by the Nernst equation for reversible reactions, whilst the overall current is zero, this is because the backward and forward current densities are equal:

$$j_0 = -j_b = j_f \tag{2.30}$$

where j_0 is the exchange current density, an important measure of the reversibility of the electron transfer reaction. By substitution therefore:

$$j_0 = nFk_f exp\left(\frac{\alpha_A nFE_e}{RT}\right) = -nFk_f exp\left(\frac{-\alpha_C nFE_e}{RT}\right) \tag{2.31}$$

Since the overall current density $j = j_f + j_b$:

$$j = k_C^{\circ} c_O exp\left(\frac{-\alpha_C nFE}{RT}\right) - k_A^{\circ} c_R exp\left(\frac{\alpha_A nFE}{RT}\right) \tag{2.32}$$

Substitution from Eq. 2.31 and defining the overpotential η as the deviation from the equilibrium potential, $\eta = E–E_e$ leads to the Butler-Volmer equation:

$$j = j_0\left\{exp\left(\frac{\alpha_A nF\eta}{RT}\right) - \left(\frac{-\alpha_C nF\eta}{RT}\right)\right\} \tag{2.33}$$

2.4.2.1 Amperometric Methods

Given the equations above, the current-voltage plot of an electrode in the presence of a single electroactive species will initially show an exponential rise as the overpotential is increased. Eventually, diffusion will start to limit the flux to the electrode surface and the current will become independent of the applied voltage. This leads to the sigmoidal form of a typical current-voltage curve illustrated schematically in Fig. 2.8.

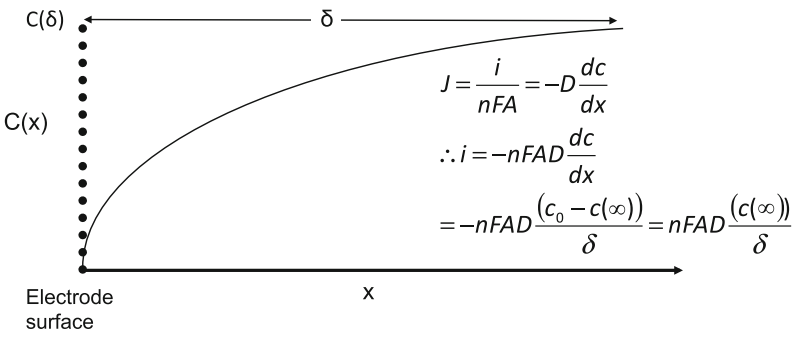

Fig. 2.9 Schematic representation of the concentration profile close in the diffusion-limited regime. Bulk concentrations are denuded close to the electrode surface, in the so-called Nernst layer. In the diffusion limited regime, the surface concentration is maintained at zero due to rapid electron transfer

In Fig. 2.8, region 1 is where the current depends on the rate of electron transfer, and is therefore potential dependent. The form of this part of the curve is given by the Butler-Volmer relationships above. In region III, the current is limited by the ability of diffusion to supply the electrode surface with electroactive material. In region 2, there is mixed control: the rates of mass transport and electron transfer are occurring at broadly similar rates. Region 3, where mass transport is limited, is the region of utility for analytical measurements since the rate of reaction, and therefore the current is proportional to the bulk concentration.

In region II, the surface concentration will be zero, since reactants arriving at the surface will be instantly oxidised or reduced. A conceptual grasp of how amperometric and voltammetric sensors can allow estimation of concentration can be got from consideration of the steady state in the diffusion limit. In this case, the concentration gradient dc/dx can be approximated by:

$$\frac{\Delta c}{\delta} = \frac{c_s - c_\infty}{\delta} \tag{2.34}$$

where c_∞ is the bulk concentration. In the diffusion limit, c_s is zero and δ is the Nernst layer thickness, that region of solution depleted by the electrode reaction. Eq. 2.25 then becomes:

$$i = -nFA\frac{c_\infty}{\delta} \tag{2.35}$$

showing that there is a linear relationship between the measured current in the external circuit and the bulk concentration. The key experimental control then is to ensure that the device is engineered so that δ is kept constant. A graphical representation of this concept is shown in Fig. 2.9.

As clearly seen, bulk movement of the solution would perturb dc/dx and therefore affect the measured current in the external circuit. This would render

the sensor useless (though this phenomenon can be exploited in constant concentration solutions to measure local mass transport rate constants).

There are three modes of mass transport: convection, migration and diffusion. In the biomedical situation, the ionic strength is such that the medium cannot support an electric field (the Debye length is around 0.5 nm) and therefore migration, the movement of a charged particle in an electric field, is not significant. Similarly, most electroanalytical experiments take place in highly conductive ionic media by design, on order to simplify the analysis. Bulk convection can be an important mass transport mechanism – diffusional speeds are of the order of 10 μm s^{-1} so any significant bulk flow will swamp diffusion. However, ultimately, the electrode surface will be in a convective boundary layer, a hypothetical thin film of stagnant solution where at physiological ionic strengths the only mode of mass transport is diffusion, described by Fick's laws. In stagnant solution at room temperature in a typical lab beaker, the boundary layer for natural convection has been estimated by Bockris to be around 0.05 cm [92]. Provided the so-called Nernst layer (that region of the solution where the analyte concentration has been significantly perturbed from the bulk value by the electrode reaction) is much smaller than the convective boundary layer then the problem can be reduced to solutions of a diffusion-reaction equation.

For a useful sensor then, the key engineering target is to ensure that δ is kept constant and ideally known, either from analytical solutions, numerical modelling or by experimental calibration. This is the case whether the applied potential is kept steady, at a potential where the electrode reaction is diffusion limited (amperometry) or systematically varied with time, as in voltammetry. There are three experimental approaches to this and all three have found application in analytical devices.

- **Forced Convection**
  Overwhelm natural convection by using a well-defined forced convection such that the convective boundary layer is significantly smaller than that due to natural convection. Examples include the rotating disc electrode which gives an analytically tractable uniform boundary within which the concentration boundary layer is entirely confined. This is a vitally important technique in sensor development as it allows decoupling of mass transport from the rate of electron transfer. However, it can only be used analytically on extracted fluid samples. Similarly, channel flow sensors can be used in the flow-injection format, again useful for high throughput analysis of multiple patient samples.
- **Membrane-covered Devices**
  This is essentially the complementary approach. A permeable membrane is applied between the electrode surface and the solution (or patient). The membrane does not permit bulk flow. Therefore, provided the diffusion coefficient of the membrane is much smaller than the solution (which will almost invariably be the case), the concentration gradient will be confined to the membrane and the external solution (or tissue) will be unperturbed by the electrode reaction. This

approach can have the additional advantage of preventing surface-active sample components from accessing the electrode surface. Examples of this approach abound in the literature. It is important to recall, however, that the current in the solution is carried by anions and cations, so the membrane must be ion permeable to provide a current path between the working and counter electrodes. This limitation is circumvented in the well-known Clark O_2 electrode, which places the entire electrochemical cell behind a gas permeable membrane, typically cellulose or PTFE. This prevents ionic access to from the test solution to the electrodes, but permits small neutral solutes such as dissolved O_2 though to react at the cathode.

- **Microelectrodes**
  If the electrode is small, the Nernst layer will be correspondingly small, For an inlaid disc microelectrode, 90 % of the diffusion gradient will be contained in a hemisphere of six times the radius of the disc [93]. Recalling Bockris' estimate of 0.05 cm as a typical natural convective boundary layer thickness and allowing a margin of one order of magnitude, a microdisc microelectrode 50 μm in diameter ought to develop a genuine diffusion limited current. This is found to be the case experimentally. Plainly, if there is bulk convective flow, the electrode would need to be smaller still. This important result has other implications. The volume of tissue sampled using a microelectrode must be of a similar dimension, so the effective spatial resolution of a microdisc electrode is also around six times its electroactive radius.

Disk microelectrodes are relatively simple to fabricate in the laboratory by insulating metal wires or carbon fibres. Sectioning with a diamond wafering saw followed by polishing with alumina slurries or diamond lapping compounds reveals the disc. Photolithographic processes can also be used but this usually leads to a recessed disc configuration due to the requirement of co-planar hook-up tracks.

Asymptotic solutions for the microdisc give the diffusion limited current [94] as:

$$i_d = 4nFcDa \tag{2.36}$$

where a is the electrode radius, c is the bulk concentration, n is the number of electrons transferred per mol. of analyte and D is the diffusion coefficient. If bare microdisc electrodes are used in vivo or in tissue samples, the diffusion coefficient is not generally known. It can however be measured in situ (using microelectrode chronoamperometry, see below) but care must be taken since D can be affected by oedema during an inflammatory response or by compression of the tissue due to the insertion of the microelectrode itself. The diffusion limited current at a recessed microdisc [95] (such as an individual element in a microfabricated microelectrode array) is:

$$i_d = \frac{4\pi nFcDa^2}{4L + \pi a} \tag{2.37}$$

it is worth noting here, that the sensitivity of devices based on microelectrodes scales linearly with the electrode radius. This gives microelectrode devices a significant scaling advantage over spectroscopic methods for miniaturisation. Spectroscopic methods essentially count molecules in a given volume so sensitivity will scale with the cube of the linear dimension.

Steady state techniques have the fastest response time of any electroanalytical technique. For electrodes without membranes, the response time is essentially instantaneous since it depends primarily on the diffusion characteristics of the test medium. Electron transfer takes place on the femtosecond time scale. It is this combination of excellent temporal resolution and unparalleled and tuneable spatial resolution that has allowed direct measurement of single vesicles of neurotransmitters to be quantified in real time; an example is detailed below. Steady state techniques offer the advantages of simple instrumentation and simple, often analytical, relationships between the measured current and analyte concentration.

In real applications however, selectivity can present a problem. Microelectrode sensors are typically tested and calibrated in homogeneous pH-buffered solutions containing only the target analyte. There is no guarantee that your biological specimen will be so obliging. In addition to the complexities introduced by compartmentalisation and inhomogeneity (outlined in the introduction above), there may be other (known or unknown) electroactive species. Selectivity in amperometric methods at bare electrode arise entirely from the applied potential. This is characteristic of the electrode material and the physic-chemical properties of the analyte (its molecular orbital energies and its energy of solvation). However, these can all be affected by pH, ionic strength and adsorption on the electrode surface, for example. So the potential identified in the calibration and characterisation may not be correct in vivo. This would not be revealed in a simple amperometric technology unless a current voltage curve was recorded at the start of the experiment, at regular intervals and at the end of the experiments. The principal problem is the presence of known or unknown interferents though. For example, in neurochemical investigations of monoamine neurotransmitters, ascorbic acid is typically present at a concentration that is 100× higher than the target analytes and are oxidisable at similar potentials. Furthermore, the monoamines have redox potentials very close to each other. Applying a steady potential at the diffusion-limited potential of, say, serotonin could result in a current that is augmented due to the unsuspected presence of dopamine, which is oxidised at a lower potential. The only way this can be tested is by running a periodic current-voltage curve or using a non-steady potential programme.

However, for the right biomedical problem, the simple instrumental requirements of amperometry and fast response times are a great advantage. All that is required is a precision voltage source; a current to voltage converter with appropriate sensitivity and some means of recording the signal. This steady applied potential also aids in applying analogue or digital filters to deionise the data.

A representative example now follows from our laboratory on the detection of serotonin release from single vesicles. We have an interest in examining the effects of ageing on release of monoamine neurotransmitters and the gaseous transmitter nitric oxide [96]. Neurotransmitters are chemical messengers which are released

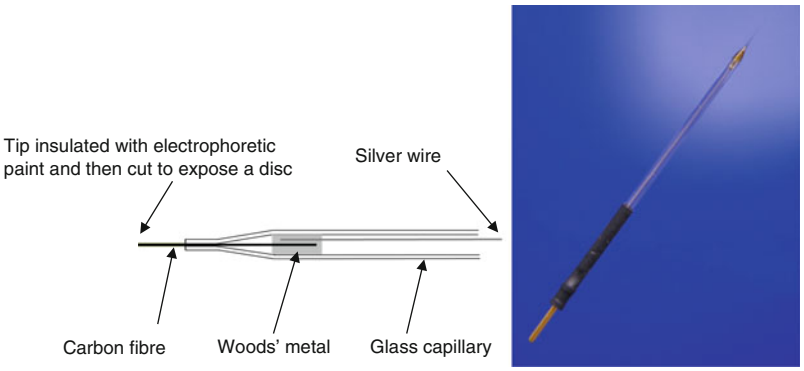

Fig. 2.10 Schematic (*left*) and photograph of a carbon fibre sensor for neurochemical application

from a pre-synaptic neuron and diffuse across the synaptic cleft where another action potential is triggered. There are three types of transmitter: gaseous e.g. nitric oxide and amino acids; peptides such as glutamate or myomodulin and monoamines such as serotonin and noradrenaline. Peptides and monoamines are released through vesicles, subcellular structures originating in the Golgi that fuse with the cell membrane and release their contents. Vesicles typically contain 20,000–50,000 molecules and the release is generally over in 5 ms. This presents a challenging measurement requirement – low concentrations, highly localised release and a requirement for excellent temporal resolution.

An example is presented on how we were able to measure serotonin (5-hydroxy tryptamine, 5-HT) release from an identified neuron in the water snail, *Lymnea stagnalis* using carbon fibre microelectrodes. The microelectrodes were fabricated as follows:

- Clean a 7 μm carbon fibre by sonication in acetone followed by deionised water.
- Place the fibre inside a pulled glass capillary (where the end as been polished to facilitate insertion). This may be aided by using a capillary filled with ethanol.
- Once placed inside the capillary allow approximately 2 mm of the carbon fibre to protrude from the end of the capillary and seal using epoxy resin by capillary action. The resin takes 72 h to set and cure at room temperature.
- Contact using a silver wire via Woods metal.
- The exposed shanks of the protruding tip are then insulated using electrophoretic paint. To coat the carbon fibre a voltage of 2 V was applied for 1 min using a platinum coil as the cathode and the carbon fibre electrode as the anode. Following coating, the electrode was removed by micromanipulator and cured. The anodic paint was then cured after each coating for 20 min at 160 °C. This process was repeated four more times and the voltage was increased to 3, 4, 6 and 8 V for each subsequent coating. The carbon fibre was then cut using a scalpel to expose a carbon fibre disc electrode.

A schematic and photograph of the completed sensor are shown in Fig. 2.10.

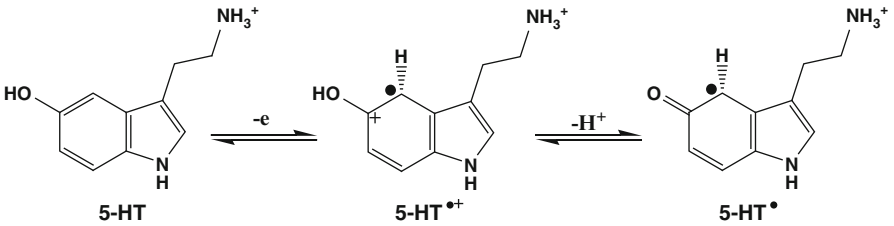

Fig. 2.11 The electrode reaction of serotonin (5-HT). The resulting radical cation is deprotonated to form the neutral radical. This can then react with unreacted serotonin or other radicals to form oligomeric or polymeric deposits on the electrode surface, leading to passivation

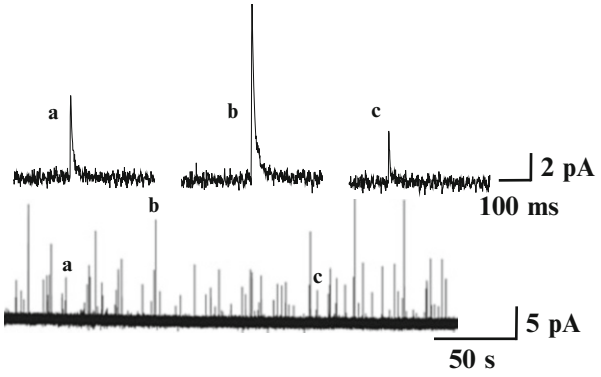

Fig. 2.12 Typical traces showing spontaneous vesicular release of serotonin from the cell body of a neuron in the intact isolated perfused CNS of *Lymnea stagnalis*. The *top trace* shows enlarged single vesicle events

The structure and electrode reaction of serotonin is given above in Fig. 2.11. When a carbon fibre electrode is polarised to +0.7 V versus an Ag/AgCl electrode (see above), it is oxidised at the hydroxyl group to a quinonoid moiety in a two-electron reaction at a rate which is proportional to its concentration.

The sensors were pressed against the surface of chosen cell of the isolated neuronal system to form, what Amatore calls, an artificial synapse [97]. Typical spiky responses are shown above (Fig. 2.12), each spike corresponding to the release of a single vesicle of neurotransmitter under the electrode surface.

The individual vesicular events are analysed for peak height, peak area (which can be related to the total number of molecules detected) and the time constant of decay, which is related to re-uptake by the pre-synaptic cell (shown schematically in Fig. 2.13).

The resolution of these recordings has been clear enough for us to detect changes in neurotransmitter re-uptake kinetics as a function of age. Key findings were that in older animals, serotonin re-uptake was inhibited to increase the peak concentration of transmitter. Similar changes were observed for nitric oxide [98], though in that case, it was the enzymes, rather than re-uptake channels that were responsible. We believe this to be an adaptive change to deal with losses of sensitivity in the post-synaptic cell in ageing. Whilst the sensor results are important on their own, an

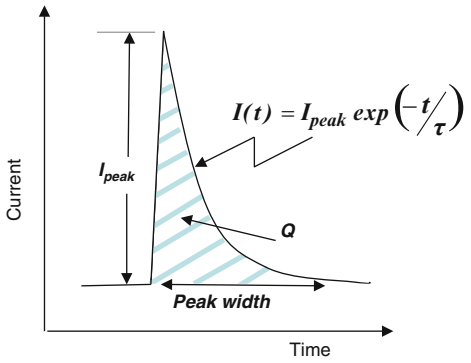

Fig. 2.13 Schematic showing the parameters extracted from each vesicle peak

important part of this work was linking the neurochemical changes to behavioural changes as the animal's age to complete the biological picture [99].

2.4.2.2 Voltammetry and the Use of Non-steady Potential Programmes

Despite the excellent spatial and temporal resolution displayed by steady state voltammetry, there are a number of disadvantages for some applications. Analyte consumption is directly proportional to current. This can be a major disadvantage in oxygen measurement where the biological problems of greatest interest occur is tissues where oxygen concentration is low. Intermittent operation can provide a solution. The limits of detection and sensitivity of the sensors are frequently limited by noise. When the currents are small, as is the case in microelectrode measurements (sub nanoamp currents are typical), the sensitivity may not be adequate. Operating the sensor with a non-steady potential increases the sensitivity by sampling the current when the concentration gradient at the surface is steeper. Operating the sensor in the steady state also raises issues of selectivity. Any molecule which can be electrolysed at or below the applied potential will contribute to the current. This is not necessarily a problem in an anatomically well characterised system, but for many applications, easily oxidisable high concentration components of most biological fluids such as ascorbate (vitamin C) or uric acid present serious problems. Potential programming can be used to confer additional selectivity. Finally, electrode fouling (of which more below in Sect. 2.5.2) can sometimes be overcome by pulsing the electrode potential either to reduce interactions or to oxidise any films formed on the electrode surface. Below, we will consider the most important transient techniques, chronoamperometry, cyclic voltammetry and square wave voltammetry. However, whilst these techniques undoubtedly overcome some problems, they introduce others, most notably capacitive charging.

When a time-varying potential is applied to an electrode, the faradaic current is accompanied by a charging current. This is not simply due to the leads and instrumentation, though these will undoubtedly contribute. The electrical double layer associated with the electrode-electrolyte interface shows capacitor-like

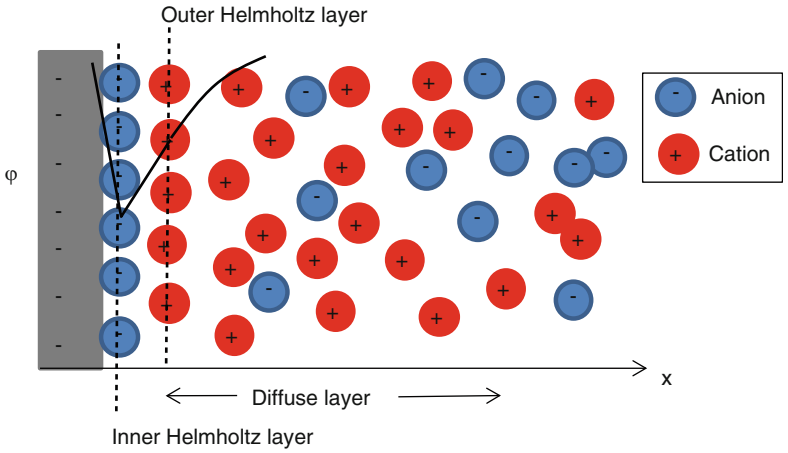

Fig. 2.14 Schematic representation of the electric double layer, the charge separation occurring at an electrified interface between an electrode and an electrolyte. The *solid black line* shows the potential varying linearly through the compact layer of adsorbed ions and exponentially in the diffuse double layer

behaviour. On the solution side of the interface there is an excess of counter ions to balance the charge on the electrode surface, a charge separation that obviously resembles a capacitor, but the charge separation is potential dependent. The dipolar water molecules are also preferentially oriented in the field. A schematic representation is shown above (Fig. 2.14).

The figure shows discrete regions where anions are specifically adsorbed (i.e. without their salvation shell) with their centres on a plane called the *inner Helmholtz layer*. Then there is an excess of solvated cations, balancing the net negative charge on the electrode. On the microscopic scale they cannot be considered as point charges, but can approach the electrode surface no closer than their hydrated radius. A plane through the centres of these ions in the compact double layer is called the *outer Helmholtz layer*. Beyond the outer Helmholtz layer, any remaining charge is balanced by a mobile *diffuse double layer*. The potential $\varphi(x)$ of the diffuse double layer in one dimension is approximated by:

$$\varphi(x) = \varphi^{\circ}\exp(-\kappa x) \tag{2.38}$$

where φ° is the potential at the surface and $1/\kappa$ is the *Debye length*, the screening length scale which depends on the ionic strength:

$$\kappa = \left(\frac{2 \times 10^3 \varepsilon^2 N^2}{\varepsilon\varepsilon_0 kT}\right) \tag{2.39}$$

The Debye length at physiological ionic strength is similar to the length of a chemical bond or a hydrated ionic radius. This matters because molecules will

barely sense the electric field until they are within a bond length and the double layer structure will, to a very good approximation, consist entirely of the inner and outer Helmholtz layer.

When the electrode potential is changed, electrical work must be done to provide the appropriate ion atmosphere and re-orientate the dipoles. This is manifested as a charging current which decays to zero in the steady state. The capacitance of a noble metal electrode is of the order of 20–30 μF cm^{-2}. Since capacitance scales with area, this problem is less severe with smaller electrodes. Some of the newer materials introduced into sensor technology, notably carbon nanotubes and boron-doped diamond, demonstrate much lower capacitance and this can offer additional advantages, though capacitance is always going to be an interference. Many of the more sophisticated and sensitive transient techniques have been designed to minimise the influence double layer charging.

The simplest transient technique is chronoamperometry. The electrode potential is instantaneously changed from one at which no electrolysis occurs, to one that sufficient enough to generate a diffusion limited current. Intermittent operation decreases analyte consumption, the electrode is polarised only when the measurement is required.

The resulting faradaic current rises instantaneously to infinity (or as fast and as high as the instrumentation will allow) as the surface concentration falls to zero. As the concentration gradient relaxes into the solution, the current decays as $t^{-1/2}$. For a large electrode, the current is given by the Cottrell equation which predicts that the current should approach zero at infinite times.

$$I = \frac{nFAc\sqrt{D}}{\sqrt{\pi t}} \tag{2.40}$$

For a disc shaped microelectrode the current asymptotes to a finite non-zero value since, as discussed above, the hemispherical diffusion field is small compared with the natural convection boundary layer. The $t = \infty$ varies with time and two asymptotic solutions exist: $\pi nFcDa$ for short times (where $4Dt/a^2 < 1$) and to $4nFcDa$ for long times [100] as the diffusion to the electrode edge increasingly dominates and the electrode begins to appear as a point sink (Fig. 2.15). The principal advantage of chronoamperometry is that since expressions for slope and intercept on the i vs. $t^{-1/2}$ plot contain both diffusion coefficient and concentration, both of these terms can be obtained from a single experiment. This is a great convenience in biological systems since the diffusion coefficient is generally unknown and likely to be different from a calibration solution. Furthermore, the diffusion coefficient is of intrinsic interest and can reflect tissue hydration. We have used this technique to quantify the effects of tissue hydration in the intervertebral disc (which is affected by mechanical loading) on oxygen transport in the tissue [101]. A further potential benefit is that it may be possible to recondition the electrode surface by applying a cleaning pulse between measurements.

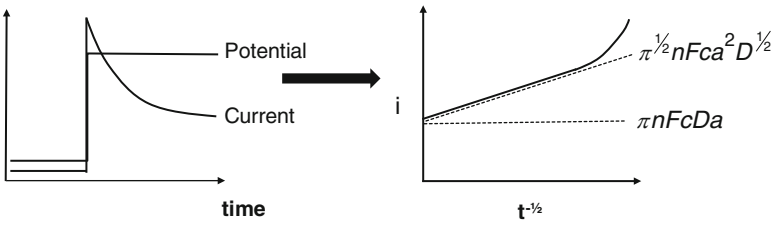

Fig. 2.15 Schematic of microelectrode chronoamperometry. The *left-hand* graph shows the potential step and the resulting current. The *right-hand* graph shows the straight-line response (after the initial capacitive charging current) and the pair of equations describing the slope and intercept

However, the early parts of the current transient are distorted by capacitive charging. The charging current goes as:

$$i(t) = \frac{\Delta E}{R} exp\left(\frac{t}{RC}\right) \tag{2.41}$$

It is essential to establish the RC time constant for charging in a blank solution and only analyse the current for times longer than $3RC$ but less than $4Dt/a^2$.

Microelectrode chronoamperometry can improve sensitivity, decrease analyte consumption (by being switched off between measurements) and give access to the diffusion coefficient independently of the concentration (which can be of critical importance in vivo, for example in the detection of oedema). However, it does not overcome the principal disadvantage of steady state techniques which is that of unknown selectivity in complex samples. Additionally, the sharp edge of the stimulating voltage can provoke action potentials in neurons. These disadvantages are to some extent overcome by other transient techniques and with modern instrumentation and there is no requirement to use only one technique.

More sophisticated transient techniques are not generally suitable for implementation in sensors, though can be useful for characterising both the sensor and the electrode reaction and assessing whether there is any couple solution chemistry occurring. Cyclic voltammetry is a particularly useful "first look" technique but, with the exception of neurotransmitter research [102, 103], has not been widely used in biosensing application due to the relatively high limits of detection of the order of 10^{-5} mol. dm^{-3} for routine applications.

Cyclic voltammetry involves applying a triangular waveform to the working electrode and plotting the resulting current as a function of the instantaneous applied potential. This is dynamic technique in that the diffusion gradient at the electrode is changing continuously with time. This results in a peak-shaped response. The peak arises when the surface concentration falls to zero. The transient current decreases with $t^{-1/2}$ (a useful check that the peak is indeed due to mass transport limitations and not to electrode fouling) as the electrode potential continues to vary. Reversing the potential scan leads to reversal of the electrode

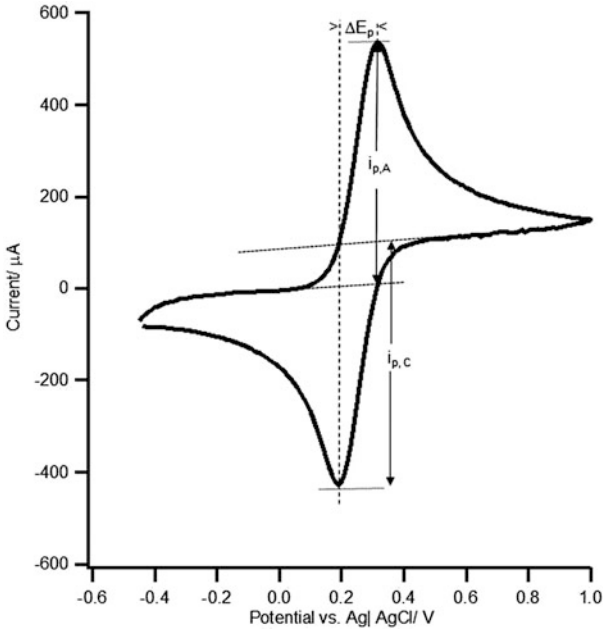

Fig. 2.16 A typical cyclic voltammogram

reaction provided that the reaction is chemically reversible in the potential range examined. A typical cyclic voltammogram (CV) is shown in Fig. 2.16.

The key parameters derived from the voltammogram are the peak currents for the cathodic and anodic reactions, $i_{p,C}$ and $i_{p,A}$; the potential separation between the two peak currents; ΔE_P and the peak width and also the potential difference between the peak current and half the peak current on the rising portion of the *i-V* curve. Diagnosis of thermodynamic reversibility is important since this dictates which form of the Randles-Sevčik equation to use. Exploitation of these equations can be important in assessing biocompatibility (see Sect. 2.5.2).

The principal roles of CV in sensor development and their applications are the characterisation of the electrode reaction and assessing the performance of the electrode. Whilst the capacitance has little analytical value, adsorption of surface-active molecules such as proteins will displace counter ions and decrease the double layer capacitance. This can be calculated directly from the CV from regions where no electrolysis is occurring – the so-called double-layer region. Since $Q = CV$, taking the time derivative gives $i = CdV/dt$. Capacitance does depend on the applied potential but changes in capacitance at any given potential are a useful diagnostic.

In neurochemical applications, the background charging currents can be orders of magnitude larger than the faradaic current. This is usually dealt with using background subtraction. The target neurochemicals are not routinely present in the milieu of the electrode, but released due to electrical stimulation as part of the

normal experimental protocol. The background current-voltage trace is a recorder prior to stimulation. There are several problems with this approach. Background subtraction involves taking the difference between two noisy digitally recorded signals, which is always problematic since the difference may be close to the resolution of the analogue-to-digital conversion. A more serious objection is the assumption that the background current is independent of the faradaic subtraction. It is inconceivable that an electrode reaction which involves adsorption prior to electron transfer and one or more proton transfers does not affect the structure of the double layer. Notwithstanding these objections, which require highly-skilled and critical understanding of the limitations of the technique, the method has led to important insights into neurochemistry which could not have been observed with other techniques.

Differential pulse voltammetry and square wave voltammetry both involve modulation of a ramp or staircase respectively with a train of square pulses. By judiciously selecting the sampling period, the effects of double layer capacitance can be substantially reduced [104]. Both of these techniques offer limits of detection down to the nanomolar but are not continuous and are difficult to implement in the clinical setting. The interested reader is referred to standard electrochemistry texts for further details. Modulating a slow-moving voltage ramp with a sine wave, a technique known as a.c. voltammetry is a promising method that has been widely underused. However, it can be easily implemented using computer controlled instrumentation and is amenable to sophisticated signal processing (see below) and new semi-analytical solutions have been presented.

2.4.3 Instrumentation

Instrumentation for potentiometry is very straightforward and this is one of the appealing aspects of potentiometric devices. A high impedance voltmeter is all that is required along with some means of recording the voltage (usually a computer) and appropriate software for scaling the voltage and relating it to the calibration working curve or prompting user actions in the method of standard additions.

Steady state amperometry, which uses active non-equilibrium potentials, requires a stable voltage source which can respond rapidly to a current load that may vary by many orders of magnitude. Most readout devices (chart recorders, oscilloscopes, analogue-to-digital converters) require the signal to be in the form of a voltage, so some sort of current to voltage conversion is required. In the case of low currents, it may be possible to use a simple two-electrode set-up where the counter electrode also serves as a reference electrode. However, passing any current through the reference electrode can reduce sensor lifetime and if an array of electrodes is to be used, the combined sensor current could cause significant current flow leading to an error in the reference electrode potential (current across an electrified interface can only be sustained by electrolysis which almost inevitably leads to a change in potential, as given by the Nernst equation (*vide supra*)) and may

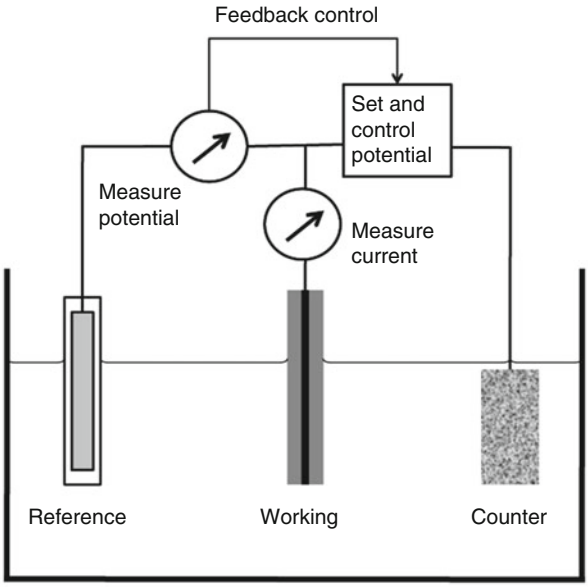

Fig. 2.17 Schematic of the instrumentation required for amperometry

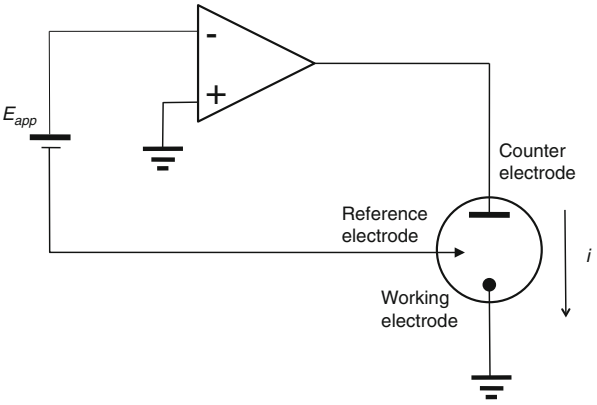

Fig. 2.18 Schematic of a potentiostat circuit based on a voltage follower

introduce hysteresis into the system. In many cases, a three-electrode set up is required. In this case, the electrode potential with respect to the reference electrode is maintained by a control amplifier and a third electrode is introduced to provide a current path. This is shown schematically in Fig. 2.17.

The functions outlined in Fig. 2.17 can be implemented using simple operational amplifier circuits. Usually, the working electrode (sensor) is held at ground or virtual ground and the potential is applied through a control amplifier to which the reference electrode and counter electrode are connected. A simple circuit for achieving this function, based on the voltage follower circuit, is shown in Fig. 2.18.

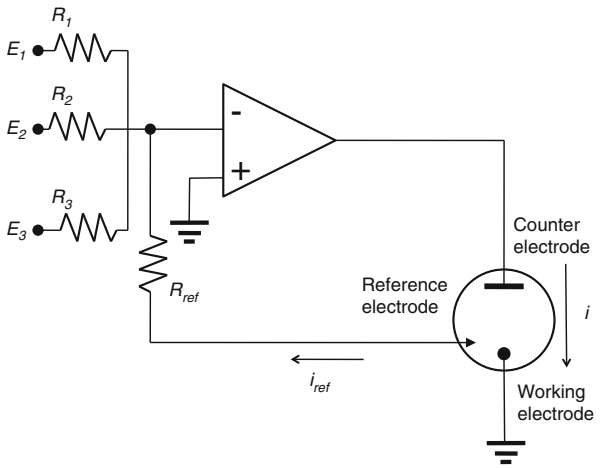

Fig. 2.19 A potentiostat based on a summing amplifier

Whilst this circuit fulfils the essential functions of the potentiostat, in that the reference electrode passes no current, it is not easily adapted for transient techniques where the voltage offset may need to be modulated with a pulse train or an a.c. voltage perturbation. In order to implement this useful function, an op-amp adder circuit can be used (Fig. 2.19):

In this circuit, the voltage applied to the electrochemical cell (or complete sensor) is given by the sum of the inputs to the three resistors (R_1, R_2, R_3), if they are of equal value. A disadvantage is that the reference electrode is now loaded by the resistor, R_{ref}. This can be easily overcome by placing a voltage follower into that limb of the circuit, between the reference electrode and $R_{ref.}$. The complete control amplifier function can now be implemented using a monolithic dual op-amp chip.

Current to voltage conversion is commonly achieved in two ways: (i) passing the current through a high precision measuring resistor and then using standard voltage amplifier circuits to provide adequate gain for interfacing to a chart recorder or analogue-to-digital conversion or (ii) a current follower. This second circuit has the advantage of holding the working electrode at virtual earth. The measuring resistor approach has the advantage of speed and low noise, but the working electrode takes a variable potential above ground. The current follower circuit maintains the working electrode at virtual earth which reduces the capacitance of the working electrode lead (the central conductor and the shield will be at the same potential) and minimises leakage currents, a major consideration when the current can be as low as picoamperes.

It is worth emphasising the advantages of applying the desired potential to the reference electrode and maintaining the working electrode at virtual earth. It is not unusual for electrochemical sensors to only produce nanoamperes or less. The applied voltage is less than 1 V. This implies an effective impedance of $>10^{10}$ Ω. Any paths to earth of less than a teraohm will cause serious errors if the working electrode is not at virtual earth. Furthermore, the non-inverting terminal can be used to drive the shield of the electrode cable further protecting signal integrity.

More recently [105], a new approach to current to voltage conversion has been employed in patch clamp amplifiers for neurophysiology. Developed by Axon, the input stage is a current integrator, thus reducing the effect of random noise. Clearly, the integrator needs to be reset periodically and the complete circuit is considerably more sophisticated and, unlike the circuits outlined above, are beyond the means of most laboratories to implement in home-made devices. Similarly, there is renewed interest in switched capacitor circuits for current to voltage conversion. Again, more sophisticated circuit analysis and design is required than is commonly available to electrochemists. These circuits have major limitations in that they are monopolar devices – the experimenter needs to select either positive or negative currents. This is less of a problem where target analytes have been identified in advance but such circuits would not be suitable for general lab use. Current integration ought to reduce noise right at the beginning of the signal processing chain. The signal is effectively digitised, though, through what is essentially a sample-and-hold circuit and it remains to be seen if these disadvantages are offset by improved signal to noise characteristics.

2.4.4 Signal Processing and Data Analysis

Although there have been tremendous advances in computing power in the last two decades, these have not thus far been translated into significant advances in the processing of data for electrochemical sensors. In fact, computers have largely been used to emulate the traditional signal generator and X-Y chart recorder approaches of half a century ago. Consequently, it is not unusual to record 50,000 pairs of data points in a cyclic voltammetry experiment only to use two or three of these in the analysis e.g. peak potential and current and half-peak potential and current. The analysis of these data then proceeds using the diagnostics developed by Nicholson and Shain in 1964 [106]. Finite difference modelling is more process intensive, but based on the same necessarily simplified models. It is used to test the similarity of the experimental data to predictions based on model reaction schemes. A major barrier is the non-linear nature of electrochemical signals which strictly precludes the use of Fourier transform approaches. Nonetheless, substantial progress has been made in using frequency space interpretations of the entire current–voltage characteristics, principally by Alan Bond and his group [107]. The approach typically involves the uses of a.c. voltammetry: a slow voltage ramp is applied to the electrochemical cell. The ramp allows a selection of the appropriate voltage for the electrochemical system of interest. Conventionally, a small amplitude sine wave is superimposed on the ramp to elicit kinetic and thermodynamic information but large amplitude perturbations provide improved signal to noise, particularly at the higher harmonics and the resulting signals have proven amenable to systematic theoretical analysis [108].

Whilst *ad hoc* modelling has undoubtedly been useful, it seems timely to apply some of the tools developed in other branches of engineering for time series analysis into electrochemistry. We have begun this process by applying the Hilbert transform to the study of immobilised redox species [109] at the surface of electrodes and have extended this work to include freely diffusing species [110, 111]. The aim of this work is to be able to deduce the thermodynamic (E°), kinetic (α, k°) and mass transport (D, concentration) parameters of all species present in solution. The combination of the physicochemical parameters ought to enable unambiguous identification and move electrochemistry away from a correlation-based approach to qualitative analysis and by altering the time scale of the experiment (by, for example, chirping the frequency) resolve redox active species that would otherwise overlap. A major advantage that is already conveyed is that the capacitance can be removed as an offset rather than through background subtraction. This is important since it is widely assumed in cyclic voltammetry that the background current is unaffected by the faradaic reaction. The Hilbert transform technique allows identification of when this cannot be true e.g. when the electrode reaction or spectator species adsorb on the electrode surface.

Furthermore, the technique can be used in reverse, to generate a digital filter that improves the selectivity of even simple devices. We were able to use optimised a.c. voltammetry waveforms to detect physiologically relevant concentrations of dopamine and serotonin (μM concentrations) [112]. These neurotransmitters are challenging to separate in voltammetry and cannot normally be distinguished using cyclic voltammetry because their peaks overlap. Conventional approaches to this problem have involved deposition of selective films on the sensors. Several other factors also complicate what is already a difficult analytical problem: ascorbate (vitamin C) is usually present at concentrations several hundred times higher than the target analytes and is also oxidised at overlapping potentials (serotonin and dopamine have formal potentials of 290 mV and 275 mV respectively); and background subtraction is not indicated since both dopamine and serotonin reaction products foul the electrode surface and displace counter ions leading to time-varying decreases in double layer capacitance. Optimisation of the potential waveform allowed simultaneous detection of serotonin and dopamine in the presence of a hundred-fold excess of ascorbate. These approaches work because although the thermodynamics properties are similar, their kinetics are different from each other and both exhibit such different kinetic characteristics from ascorbate that appropriately optimised waveforms can emphasise one reaction over another. The application of digital signal processing to electroanalysis is currently in it infancy. However, the preliminary results demonstrate their potential in improving analyte identification (through unambiguous determination of the characteristic physicochemical parameters) and improving the selectivity of simple easy-to-make sensors (Fig. 2.20).

New semi-analytic asymptotic solutions for a.c. voltammetry for surface confined species [113] and freely-diffusing species [114] have recently been reported and hold out the prospect of more rational exploration of system parameters.

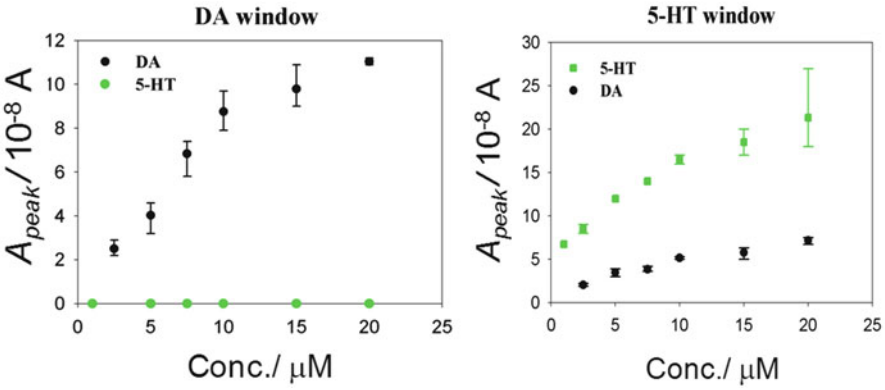

Fig. 2.20 Calibration curves for dopamine and serotonin (5-HT) using the amplitude extracted using the Hilbert transform response. The potential ramp was sine modulated at 150 Hz with an amplitude of 0.4 V. Dopamine and serotonin were distinguished by the choice of ramp potential. Ascorbate interference was removed using the high frequency and high amplitude modulation

2.5 Multiple Sensors and Microsensor Arrays

Microelectrode arrays offer advantages for bioanalysis. These advantages accrue from several sources relating to both the properties of living tissues and the understandable wish to measure more than one analytical variable. Firstly, one of the governing characteristics of living tissues is the large variability from site to site, on whatever length scale. This is discussed in the introduction above. Many disease processes, notably cancer, arise from the aberrant behaviour of one or a few cells. The central value obtained from averaging over a large number of cells will therefore be barely affected, however, the range of values will change. Given the widely differing range of analyte concentrations found in biology, for example the prostate cancer marker PSA, it is likely that the variance is at least as interesting as the central value. Such concepts are likely to be of value in personalised medicine.

Many of the target analytes in bioanalysis are surrogate variables that statistically correlate with the diagnostic target. Measuring more than one analyte or biomarker greatly adds to the confidence and may generate new insights into the underlying molecular mechanisms of disease. For example, simultaneous measurement of pH and histamine concentrations in isolated perfused stomach have elucidated the relative importance of the signalling pathways controlling acid secretion [67] and we have extended this technology to the array format [68].

Microelectrode arrays for recording from brain slices, cultured cells or even from in vivo preparations have been described for many years. Some of these are commercially available (Microchannel Systems GmbH, Ayanda Biosystems, 3Brain etc.). On the face of it, these ought to be easily adapted for electroanalysis – after all, all you really need is an array of inert, individually addressable conducting pads

of suitable dimensions. CMOS processing is mature technology and, in principle, allows for integrated electronics. Consequently, it is tempting to adapt for the apparently simple problem of generating massively parallel microelectrode arrays [115]. However, several problems are immediately evident. The materials used in conventional CMOS processing [116] are rarely suitable for biological applications. Ionic contamination is a major problem and extensive (and expensive) post-lithographic processing using hafnium or platinum, for example, is usually required [117, 118]. Conventional planar photolithography leads to recessed electrode geometry (unless two additional layers are used followed by chemical-mechanical lapping). The electrode hook-up tracks are usually insulated with <1 μm silicon nitride or oxide. Such thin dielectric allows some leakage of the electric field into the test specimen and will contribute to much larger capacitance than observed for conventional microelectrode sensors. This can cause problems with dynamic techniques where the *i-V* characteristics will be dominated by charging currents.

The principal area of failure for all microelectrodes is the metal-insulator seal. Such failures, often arising from unresolved thermal stresses, lead to hairline cracks, often of μm dimensions. Such failures lead to hysteresis and sluggish responses to changes in concentration. These defects can be hard to detect from conventional characterisation, e.g. measurement of the diffusion limited current, because the spatial resolution is of the order of $(2Dt)^{1/2}$ where D is the diffusion coefficient and t is the timescale of the experiment. Since D is around 10^{-10} m^2 s^{-1} and is at a steady state, the *i-V* curve takes around 100 s to record and asperities and defects less than 0.1 mm may not be evident. More rigorous testing procedures are described below. Such tests are not yet standard in the literature and this has led to over-optimistic conclusions in many cases.

Biocompatibility is the other major problem. Many devices reported in the literature are tested with cancer cell lines rather than primary mammalian cells. This is a very poor test for biocompatibility since one of the key characteristics of cancer cells is their ability to grow. Again, this has led to undue optimism about the suitability of many published devices. The other side of biocompatibility is the ability of the sensor to function in the presence of surface active spectator species. There are surprisingly few reports of sensor arrays being used in cell culture medium, the majority being reported in medium free buffer solutions. Most worryingly, some are reported in phosphate-buffered saline which will precipitate Ca^{2+} ions. Genuinely biocompatible sensor arrays are described below, along with rigorous tests for evaluating their performance.

It may be that processes designed for semiconductor microfabrication may be less than suitable for biosensor fabrication. After all, when solid state electronics came along, the manufacturing processes were developed from the ground up and not adapted from vacuum tube technology. A recent paper [119] describes the production of carbon-ring microelectrode arrays prepared from the pyrolysis of acetylene, which, though craft-intensive, could potentially be automated, and the production could thus be scaled up. Compton et al. have published a useful review [120] of fabrication methods, theoretical descriptions and characterisations.

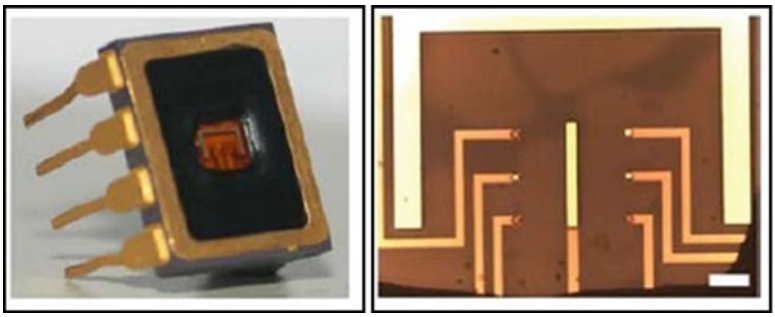

Fig. 2.21 DIL packaged microelectrode array (*left*) and a close up of the 4 mm × 4 mm sensing area

2.5.1 *Microelectrode Arrays for Primary Mammalian Cell Culture*

Over a series of papers, we have described the development of microelectrode arrays to measure signalling molecules. The devices come in two formats: a DIL package [121], and a more recently developed device based on transparent SiO_2 to enable simultaneous observation by light microscopy (see below). The DIL device (Fig. 2.21) was connected to the pins using wire-bonding. The SiO_2 based devices are connected via spring-loaded pins to a Faraday cage (Fig. 2.22) which has a temperature control (using a Peltier device with PID control implemented in LabView) to better than ±0.1 °C.

The devices are development platforms which can be post processed in the laboratory to alter the range of analytes. As bare gold, the arrays can detect nitric oxide (or more generally NO and NO_2^-) using differential pulse voltammetry (DPV) with a peak potential around +0.8 V and dissolved O_2 and hydrogen peroxide with peak potentials around −0.5 and −0.8 V respectively. Modification with iridium oxide (*vide supra*) gives an array of pH sensors and modification with oxidase enzymes and polyphenol allows detection of nutritional markers such as glucose or lactate.

The key to utilising these devices, however, is the biocompatibility from the cellular perspective and extensive physicochemical characterisation in the presence of biological components to test whether the sensors are still working. After a comparison of several different coating materials [122], air-dried fibronectin was shown to have superior properties both for cell culture and for maintaining sensor function over several days in the cell culture. Rehydrated fibronectin has a structure resembling female Velcro (see Fig. 2.23). This is likely to be due to the cysteine groups being well spaced in fibronectin leading to pores which barely affect the accessibility of the sensor surface for small molecules, but effectively repel albumin or exclude albumin or other surface active biopolymers.

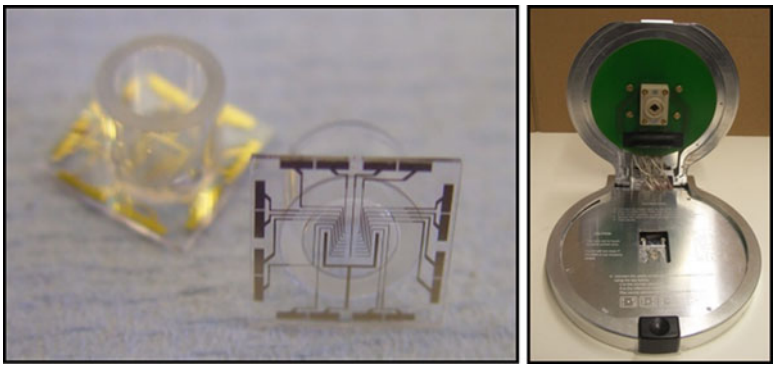

Fig. 2.22 The SiO_2-based array (*left*) and the sprung pin connecting Faraday cage for recording

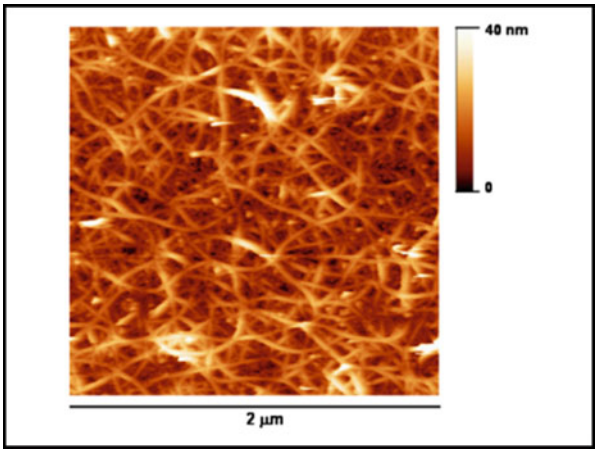

Fig. 2.23 Atomic force micrograph of air-dried fibronectin

2.5.2 Assessing Biocompatibility

An excellent introduction to the seemingly intractable problem of biocompatibility for implantable biosensors and chemical sensors has been published by Vadgama [11] and good reviews for all of the processes involved are covered by Meyerhoff [123].

Morais et al. [124] review the problems specific to implantable glucose sensors: the closed-loop operation of glucose sensors still seems an unsolved engineering challenge, though much progress has been made in recent years. New approaches to long-term biocompatibility of implanted devices have emerged: getting the sensor to integrate into the living tissue after decades of research, where the paradigm has been precisely the opposite, seems like a promising research avenue. These new approaches are in their infancy but include ambitious ideas, even to the extent of encouraging vascularisation by local infusion of vascular endothelial growth factor

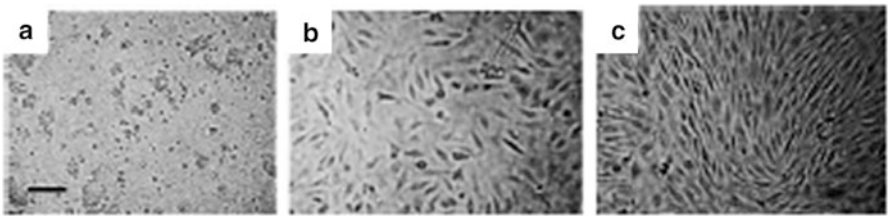

Fig. 2.24 Primary porcine endothelial cells grown on PSS-PLL (**a**), for 24 h (**b**) and 48 h (**c**) on air dried fibronectin coated polystyrene

(VEG-F) [125] or, even more radically, incorporating engineered cells expressing VEG-F into the sensor implantation site [126]. Such radical approaches are unlikely to achieve regulatory approval, but demonstrate the feasibility of incorporating the sensor into the patient. Synthetic constructions able to exploit similar signalling pathways would seem like an important next step.

For our in vitro devices, the problems are less severe and are largely to do with (i) the effects of the sensors on delicate cultured primary mammalian cells and (ii) the effect of culture medium components on sensor performance. We have taken the unusual step of considering both aspects to be important. Furthermore, We have also developed a protocol for rapid testing of biosensors for the likely ability to perform in the presence of biological systems. Firstly, examine the effects of 4 % (w/w) albumin. This is the same concentration of albumin that is found in plasma. Secondly, the rather savage 20 % emulsified chicken liver suspension. Examine the *i-V* characteristics. Key parameters are capacitance, peak width and peak separation. These are discussed in some detail, after we've decided what the sensors do to the cells.

- **What do the devices do to the cells?**
  Primary endothelial cells are adherent and, when healthy, have a characteristic elongated shape. Comparison between fibronectin and the putatively biocompatible synthetic copolymer polystyrene sulphonate-poly-L-lysine (PSS-PLL) is shown above (Fig. 2.24). After 48 h the cells on the fibronectin have grown to confluence and look healthy. In comparison, the cells on the PSS-PLL substrate almost literally curl up and die.
- **Does applied potential affect the cells?**
  We do not expect the electric potential to affect the cells directly because the Debye length, the shielding length scale for the electric field (*vide supra*), in the culture medium is less than 1 nm. However, negative electric potentials could lead to increased pH particularly due to O_2 reduction and, at extreme potentials, hydrolyse the water to form hydrogen. Similarly, at positive potentials, the solution in the vicinity of the electrode will increase if the water is electrolysed to oxygen. Depending on the electrode material, this would be expected to occur for potentials higher than around +1.0 V. We examined these possibilities on a transparent microelectrode array where cultured cells were exposed to different potentials for five minutes. The cells were then exposed to Trypan blue, a dye

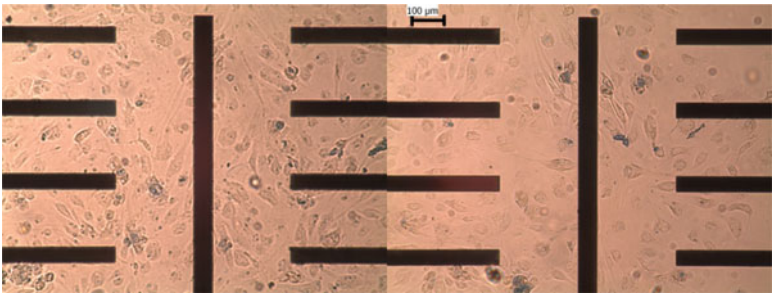

Fig. 2.25 Endothelial cells exposed to +1.5 V (*left*) and −1.0 V (*right*) (The pictures were taken from R. Trouillon, PhD thesis, Imperial College 2010)

which is only taken up by dead cells. Representative results are shown above (Fig. 2.25).

These results show some cell death, presumably due to pH changes close to the electrodes for potentials higher than 1.0 V and lower than −1.0 V.

- **What happens to the electrodes?**
  Adsorption of surface active biomolecules or deliberately added electrode modifiers might be expected to do several things to an electrode: hinder diffusion, inhibit electrocatalysis and affect the partitioning or solubility of the analyte. The effects on diffusion can be quantified using a reversible outer sphere electron transfer couple such as ruthenium (III) hexaammine, $Ru(NH_3)_6^{3+}$. Outer sphere redox is the simplest possible electron transfer process where no bonds are broken or formed and there is no adsorption of reactant or product. Reversibility means that the electron transfer is essentially instantaneous on the time scale of the experiment. Examination of the cyclic voltammograms shows that the peak width is consistent with reversibility (Fig. 2.26a).

  The peak current intensity is however decreased due to a decreased diffusion coefficient in the vicinity of the electrode.

  Adsorption, where the polymer forms an intimate relationship with the electrode surface, would be expected to show several effects: firstly, the capacitance would decrease as the counter ions are displaced by adsorbate. This can be assessed from a.c. impedance measurements by fitting the data to the Randles' model [48] or simply from the so-called double-layer region of the voltammogram:

$$Q = CV \therefore \frac{dQ}{dt} = i = C\frac{dV}{dt} \tag{2.42}$$

assuming the capacitance does not depend on potential (this is definitely not a good assumption, but big changes in capacitance are readily apparent and semi-quantitatively positive for these kind of measurements). Secondly, since adsorption is spontaneous, the free energy must be negative. Inevitably this means that surface sites, which are important for electrocatalytic reactions (where the analyte is

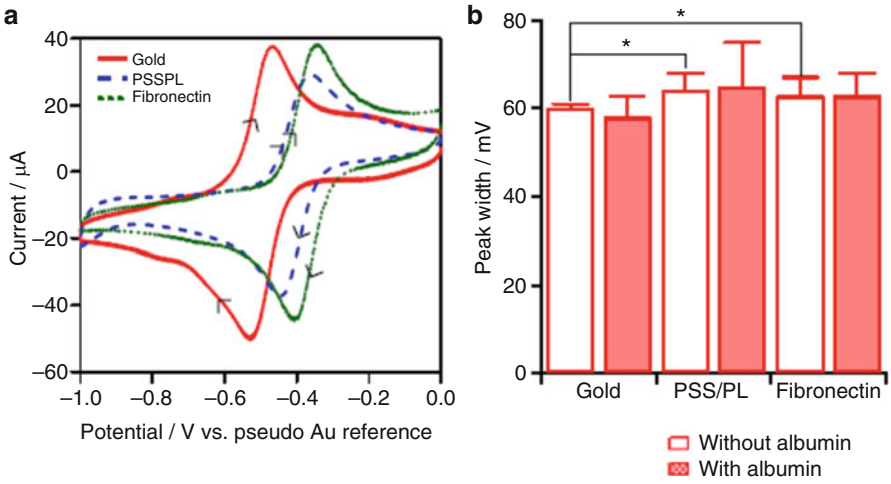

Fig. 2.26 Cyclic voltammograms examining the effect of surface coatings and exposure to albumin

adsorbed before electron transfer, e.g. O_2 reduction), will also be selectively hit by adsorption from proteins. These effects will show up in the peak width in particular or in measurement of the charge transfer resistance from a.c impedance measurements. It was this more rigorous testing that led to the conclusion that fibronectin is the preferred coating material – measurement of dissolved oxygen in fibronectin-coated electrodes though affected by the fibronectin, were not affected by albumin or chicken liver [127].

- **How big are my sensors?**
  This is a non trivial question whose answer depends on the relevant length scale, much in the same way as the measurement of the coastline of Great Britain depends on whether one measures round every single pebble on Brighton beach. Plainly, a sensible answer is required for proper quality control of microfabrication processes and to enable optimisation of the potential waveforms and associated amplification and data processing. Atomic scale measurements of the surface area will, unless the electrode is atomically flat, give larger areas than micrographs or measurements of the diffusion limited current. As mentioned above, the length scale for diffusion-based measurements will be of the order of $(2Dt)^{1/2}$. Measurement will then be no better resolved than a few tens of micrometres in most instances. This becomes a problem when one wishes to assess whether the electrode-insulator seal is intact, whether polishing has worked and if the nanoparticles used in electrode modification have actually deposited successfully in ohmic contact. For measurements based on capacitance, the resolution will be on the scale of the Debye length. This can be a rapid and convenient semi-quantitative measurement. However, accurate determination depends on there being reliable estimates of the specific capacitance of your electrode material in the electrolyte of choice. More reliable techniques for gold

electrodes involve measuring the area of gold oxide reduction peak. This peak area, conveniently generated during the electrochemical cleaning of the electrode in sulfuric acid (0.1 M) and presented in *i-t* form, can be related to near atomic scale area since 390 μC cm^{-2} of charge is passed on during its reduction [128]. Similar approaches can be employed for Pt electrodes, this time using the known unit cell size of β-hydride peaks and Faraday's law.

The meaning of electrode area is discussed in some detail in a report [129] prepared for the International Union of Pure and Applied Chemistry (IUPAC). This report is also an excellent source and critical review of methods commonly used to assess electrode area.

- **What can we use the arrays for?**
  We have used these devices to look at endothelial cell responses to angiogenin [130] and other growth factors [131]. The multiple sensor format has allowed signal averaging and real estimation of the range of cellular responses to stimulation. Because the devices were mass produced (using conventional lift-off processes), we were able to run many experiments in parallel and use well-established drugs to demonstrate the intracellular pathways in nitric oxide release. More recently we have applied similar technology to the study of host-pathogen interactions, specifically the release of nitric oxide from macrophages exposed to the protective antigen from *Bacillus anthracis* [132]. The potential for parallel experimentation and near real time and quantitative data offer significant advantages over fluorescence microscopy and enable interrogation of intracellular pathways.

2.6 New Materials

Several new materials have emerged in recent years that have great potential as sensor materials. In particular, novel forms of carbon including boron-doped diamond (BDD), carbon nanotubes (CNTs) and graphene have all been investigated for the properties as electrode materials.

Boron-doped diamond (BDD) is produced using P-CVD processes and retains many of the attractive properties of intrinsic diamond – high thermal conductivity, chemical inertness, lubricity – whilst doping at high levels ($[B] > 10^{20}$ cm^{-3}) leads to metallic conductivity [133]. A particularly attractive property of BDD is its relative resistance to the adsorption of either electrode reaction products or surface active biomolecules, presumably due to the sp^3 hybridisation of the carbon which leaves no opportunity to accept or donate electrons. Its resistance to adsorption has been compared favourably to glassy carbon [134] and the effects of doping levels on biocompatibility have been documented [135]. The wide potential window of BDD is another unique property. In principle this ought to mean that a wider range of analytes is available since hydrogen generation or oxygen generation at the negative and positive potential limits respectively, are hindered due to the non-electrocatalytic properties. In practice, however, the advantages of this wide

potential window have largely failed to be realised since many target analytes also depend upon an electrocatalytic electrode mechanism. Nonetheless, the low capacitance and long-term stability augur well for major applications in bioanalysis and environmental application. Electroanalytical applications of BDD in biology were reviewed by Swain [136, 137] and there have been important accounts of BDD in hostile environments such as the gut [138].

Much of the early work on BDD was hampered by poor reproducibility of the starting material and variable surface pre-treatments used by different investigators. The role of sp^2 impurities, grain boundaries, heterogeneities and terminating groups on the surface has now been elucidated using highly local measurements in a recent paper by Macpherson [139]. This has greatly clarified the important technical issues, identified the key parameters for electroanalysis and, in collaboration with Element 6, has led to reproducible commercially available electroanalytical grade BDD.

Carbon nanotubes are another promising material for electroanalysis. Their extraordinary mechanical properties, ballistic conductance in a large fraction of fibres and anomalously low capacitance make them attractive for biological applications. The tiny size (an astonishing 1–3 nm in diameter for pristine single-walled nanotubes) also holds out the possibility of highly localised measurements. Again, similarly to the early BDD work, considerable variation in performance is reported in the literature. In this instance, the role of catalyst impurities [140] (usually transition metals) was widely unrecognized in early reports. This was further confounded by the use of oxidizing reagents such as nitric acid which introduce oxygen functionality at the edge and break the nanotubes into smaller fragments. All of these factors affect the electrochemical performance. The role of the thin film behaviour of nanotube-modified electrodes also confounded early interpretations [141]. These early controversies are summarised and resolved in a good review [142]. Nanotube mats or sparse networks have been prepared using photoresist to mask of the catalysts. These pristine single walled nanotube devices allow the exploration of the unique properties of the nanotubes themselves. At a high density, the mats behave like complete metal films, despite the nanotubes occupying only a low percentage of the surface [143]. This gives very low capacitance, very high rates of mass transport and the ability to detect nanomolar concentrations using simple techniques such as cyclic voltammetry as demonstrated for the biologically significant serotonin [144]. In addition to their direct use as sensors, carbon nanotubes can also be used to template other materials [145] and have even been suggested for implantable devices [146].

Graphene is a relative newcomer to electrochemistry, though the subject of intense investigation. Again, purity and condition of the source material are confounding factors in interpreting some of the prematurely published accounts. The electrochemical properties of well-characterised graphene, free from copper contamination do not seem to differ greatly from basal plane graphite, though the high conductivity and optical transparency may offer advantages in some applications. Electrochemical applications have been recently reviewed [147] and applications in field effect transistor sensors have been reported [42].

2.7 Future Perspectives and Research Challenges

The goal of implantable complete devices comprising of sensors, instrumentation, signal processing, power and wireless data transmission remains in the future, but substantial progress continues to be made. Obviously, such complete devices will require new ways of thinking about the other key components, apart from the sensors. Batteries remain the most likely technology and power harvesting or other approaches remain research topics. Battery form is important and the ability to mass manufacture, or scale-up lab-based technology is critical. Recent progress has been reported for the Finnish-developed 'Enfucell softBattery' based on $Zn\text{-}MnO_2\text{-}ZnCl_2$ robust chemistry which is now commercially available in a suitable size (0.7 mm thick, the smallest is 42 × 60 mm), in a 10–90 mAh capacity and manufactured using reel-to-reel processes along with a 1–2 year shelf life. A device has been reported that is fabricated from materials described by the authors [148] as "completely edible" though more fastidious diners may baulk at silver nanowires and poly(glycerol-co-sebacate)-cinnamate. Graphene probably has more potential as a power source component than sensor [149], though the way forward may be metal-free and an all polymer PEDOT device has been reported [150].

Cheap, printable flexible displays are also an active research area. Electrochromic displays on PET substrates using organic transistors have been described consisting with demonstration of an 8 × 8 pixel display manufactured using solution processing based on standard printing and coating [151].

System integration remains the 'holy grail' but is still rarely reported, presumably because of the skill mix required for implementation transcends traditional disciplinary boundaries and the engineering problems remain significant on all aspects, ranging from biocompatibility and sensor stability (probably the most difficult challenge), through to power management, wireless data transmission and presentation of the data in a clinically meaningful form. A complete implantable device [152], the Nano-tera i-IronIC has recently been reported by de Micheli (from EPFL) at the DATE13 conference. At only 14 mm long, it consists of five sensors and a radio transmitter. The device is implanted just below the skin with an external 0.1 W battery patch. Peer-reviewed publication is eagerly awaited to see if the science lives up to the press release.

There continues to be major advances in biosensors for biomedical application. Whilst we now have a better understanding of long-standing problems of poor biocompatibility of typical sensor materials and poor stability of implanted devices, there are no magic bullets and the interface between the sensor and the biology remains the major problem. New materials, in particular, present both new opportunities and new challenges. Array technology offers a broader range of analytes, better stability through sensor redundancy and a better understanding of the role of analyte variance in biology.

References

1. McDonagh C, Burke CS, MacCraith BD, 'Optical chemical sensors' *Chem. Rev.* 108 400–422 (2008).
2. Turner APF, 'Biosensors: sense and sensibility' *Chem. Soc. Rev.* 42 31284–3196 (2013).
3. Moore FA, McKinley BA, 'The next generation in shock resuscitation' *Lancet* 363 1988–1996 (2004).
4. Sanders GHW & Manz A, 'Chip-based microsystems for genomic and proteomic analysis' *Trac Trends in Analytical Chemistry*, 19(6) 364–378 (2000).
5. Lander ES 'The new genomics: global views of biology' *Science* 274 5287 (1996).
6. Nielsen J and Oliver S 'The next wave in metabolome analysis' *Trends in Biotechnology* 23(11) 544–546 (2005).
7. Croston GE 'Functional cell-based uHTS in chemical genomic drug discovery'. *Trends in Biotechnology* 20(3) 110–115(2002).
8. Dittrich PS and Manz A, 'Lab-on-a-chip: microfluidics in drug discovery' *Nature Reviews Drug Discovery* 5(3): p. 210–218 (2006).
9. Wunberg T, et al., 'Improving the hit-to-lead process: data-driven assessment of drug-like and lead-like screening hits' *Drug Discovery Today*,. 11(3–4) 175–180 (2006).
10. Hong J, Edel JB and deMello AJ, 'Micro- and nanofluidic systems for high-throughput biological screening'. *Drug Discovery Today* 14(3–4)134–146 (2009).
11. Vadgama PM, Schoeleber in P.N. Bartlett (ed.) 'Bioelectrochemistry: fundamentals, experimental techniques and applications' Wiley 2008, Chapter 13.
12. Seo J-H, Leow PL, Cho S-H, Lim H-W, Kim J-Y, Patel BA, Park J-G & O'Hare D, 'Development of inlaid electrodes for whole column electrochemical detection in HPLC' *Lab on a Chip* 9 2238–2244 (2009).
13. Malinski T & Taha Z, *Nature* 358 676–678 (1992).
14. Updike JW & Hicks JP, *Nature* 214 986–988 (1967).
15. Bartlett PN & Caruana DJ, *Analyst* 117 1287 (1992)
16. Khurana M.K, Winlove C.P & O'Hare D. 'Detection Mechanism of Metallised Carbon Epoxy Oxidase Enzyme Based Sensors' *Electroanalysis* 15 1023–1030 (2003).
17. Barker SA in Turner APF *et al.* (eds.) *Biosensors: Fundamentals and Applications* Oxford University Press, Oxford 1987. Ch. 6.
18. Willner I, *Science* 229 1877 (2003).
19. Cass AEG, Davis G, Francis GD, Hill HAO, Aston WJ, Higgins LJ, Plotkin EV, Scott LD & Turner APF, *Anal. Chem.* 56 657 (1984).
20. Bartlett PN & Bradford VQ, *J.C.S. Chem Comm.* 16 1135–1136 (1990)
21. Zhao S, Korell U, Cuccia L & Lennox RB, *J. Phys. Chem.* 96 5641–5652 (1992).
22. Boutelle MG, Stanford C, Fillenz M, Albery MJ & Bartlett PN, *Neuroscience. Lett.* 72 283–288 (1986).
23. Ye M, Hammerle AJJ, Olstehoorn W, Schumann W, Schmidt AK, Duine JA & Heller A, *Anal. Chem.* 65 238 (1993).
24. Heller A *et al. Acc. Chem. Res.* 23 128 (1990).
25. Song KM, Lee S, Ban C, 'Aptamers and Their Biological Applications' *Sensors* 12 612–631 (2012).
26. Fodey T, Leonard P, O'Mahony J. *et al.* 'Developments in the production of biological and synthetic binders for immunoassay and sensor-based detection of small molecules' TRAC-Trends in analytical chemistry 30 254–269 (2011)
27. Iliuk AB, Hu L, Tao WA, 'Aptamer in Bioanalytical Applications' *Anal. Chem.* 83 4440–4452 (2011).
28. Ellington AD & Szostak JW '*In vitro* selection of RNA molecules that bind specific ligands' *Nature* 346 818–22 (1990).
29. Liu J, Cao Z, Lu Y, 'Functional nucleic acid sensors' *Chem. Rev.* 109 1948–1998 (2009).

30. Tombelli S, Minunni A & Mascini A, 'Analytical applications of aptamers' *Biosensors & Bioelectronics* 20 2424–2434 (2005).
31. Liu, Y, Matharu Z, Howland MC, Revzin A & Simonian AL 'Affinity and enzyme-based biosensors: recent advances and emerging applications in cell analysis and point-of-care testing' *Anal. Bioanal. Chem.* 404 1181–1196 (2012)
32. Zhou J, Battig M R, Wang Y, 'Aptamer-based molecular recognition for biosensor development' *Anal. Bioanal. Chem.* 398 2471–2480 (2010)
33. Palchetti I & Mascini M 'Electrochemical nanomaterial-based nucleic acid aptasensors' *Anal. Bioanal. Chem.* 402 3103–3114 (2012).
34. Yano K, Karube I *TRAC Trends Anal Chem* 18 199–204 (1999).
35. Shimizu KD, Stephenson CJ *Curr. Opin. Chem. Biol.* 14 743–750 (2010)
36. Suryanarayanan V, Wu C-T, Ho K-C *Electroanalysis* 22 1795–1811 (2010).
37. Malitesta C & Mazzotta E, Picca RA, Poma A, Chianella I & Piletsky SA, 'MIP sensors – the electrochemical approach' *Anal. Bioanal. Chem.* 402 1827–1846 (2012).
38. Wang X-D. & Wolfbeis OS, 'Fiber-Optic Chemical Sensors and Biosensors (2008–2012)' *Anal. Chem.* 85 487–508 (2013)
39. Stewart MER, Anderton LB, Thompson J, Maria SK, Gray JA, Rogers & RG Nuzzo 'Nanostructured plasmonic sensors' *Chem. Rev.* 108 494–521 (2008)
40. Kergoat L, Piro B, Berggren M, Horowitz G & Pham M-C 'Advances in organic transistor-based biosensors: from organic electrochemical transistors to electrolyte-gated organic field-effect transistors' *Anal. Bioanal. Chem.* 402 1813–1826 (2012).
41. Goeders KM, Colton JS, Bottomley LA, 'Microcantilevers: Sensing Chemical Interactions via Mechanical Motion' *Chem. Rev.* 108 522–542 (2008).
42. Stine R, Mulvaney SP, Robinson JT, Tamanaha CR & Sheehan PE, 'Fabrication, Optimization, and Use of Graphene Field Effect Sensors' *Anal. Chem.*, 85 509–521 (2013).
43. Kim DJ, Sohn IY, Jung JH, Yoon OJ, Lee NE, Park JS 'Reduced graphene oxide field-effect transistor for label-free femtomolar protein detection' *Biosens Bioelectron.* 41 621–626 (2013).
44. Kwak YH. Choi DS, Kim YN, Kim H, Yoon DH, Ahn S-S, Yang JW, Yang WS, Seo S 'Flexible glucose sensor using CVD-grown graphene-based field effect transistor' *Biosens. Bioelectron.*, 37, 82–87 (2012).
45. McKinley BA, 'ISFET and fiber optic sensor technologies: in vivo experience and critical care monitoring', *Chem. Rev.* 108 826–44 (2008)
46. Kimmel DW, LeBlanc G, Meschievitz ME, and Cliffel DE 'Electrochemical Sensors and Biosensors' *Anal. Chem.* 84 685–707 (2012).
47. Pletcher D 'A first course in electrode processes' 2nd ed. Royal Society of Chemistry, Cambridge 2009.
48. Bard AJ & Faulkner LR 'Electrochemical methods: fundamentals and applications' 2nd ed. Wiley, Chichester 2001.
49. Kissinger P & Heineman WR, 'Laboratory techniques in electroanalytical chemistry' 2nd ed. Marcel Dekker, New York 1996.
50. Pletcher D, Greff R, Peat R, Peter LM, Robinson J, Woodhead Publishing, Cambridge 2001.
51. Purves RD, 'Microelectrode methods for intracellular recording and ionophoresis' Academic Press, London 1981.
52. Amman D, 'Ion-selective microelectrodes: Principles, Design and Applications' Springer-Verlag: Berlin, 1986.
53. Voipio J. In 'pH and Brain Function' Kaila, K., Ransom, B. R., (Eds.) Wiley-Liss: New York, 1998; p 95.
54. Takahashi A, Camacho P, Lechleiter J, 'Measurement of intracellular calcium' Herman, B. *Physiol. Rev.* 1999, *79*, 1089.
55. Cremer M, 'Über die Ursache der elektromotorischen Eigenschaften der Gewebe, zugleich ein Beitrag zur Lehre von Polyphasischen Elektrolytketten.' *Z. Biol.* 47 56 (1906).

56. Idegami K, Chikae M, Nagatani N, Tamiya E, Takamura Y, 'Fabrication and Characterization of Planar Screen-Printed Ag/AgCl Reference Electrode for Disposable Sensor Strip' *Jpn. J. Appl. Phys.,* 49 097001–097003 (2010).
57. Park WJ, Yi Y, Lee J, Lee BC, Park OK, Lee HJ, Lee H, 'N-heterocyclic carbene–silver complex as a novel reference electrode in electrochemical applications' *Talanta* 81 482–485 (2010).
58. Noh J, Park S, Boo H, Kim HC, Chung TD 'Nanoporous platinum solid-state reference electrode with layer-by-layer polyelectrolyte junction for pH sensing chip' *Lab on a Chip* 11 664–671 (2010).
59. Capone S, A de Robertin, C de Stefano, & Scarcella R, 'Ionic strength dependence of formation constants X. Proton activity coefficients at various temperatures and ionic strength and their use in the study of complex equilibria', *Talanta* 34 593–598 (1987).
60. Fedirko N, Svichar N, & Chesler M, 'Fabrication and use of high speed concentric H+ and Ca^{2+} selective microelectrodes suitable for *in vitro* extracellular recording' *J. Neurophysiol.* 96, 919. (2006),
61. Ujec E, Keller O, Machek J, and Pavlik V. Low impedance coaxial K+ selective microelectrodes. *Pfluegers Arch* 382 189–192, 1979
62. Ives DJG in "Reference Electrodes" D.J.G. Ives & G.J. Janz (eds.) Academic Press, New York, 1961, Chapter 7.
63. Głab S, Hulanicki A, Edwall G & F Ingman, 'Metal-metal oxide and metal oxide electrodes as pH sensors' *Crti. Rev. Anal. Chem.* 21 29–47 (1989).
64. O'Hare D, Parker KH & Winlove CP "Metal-metal oxide pH sensors for physiological application" *Medical Engineering & Physics* 28 982–8 (2006)
65. Haggard HW & Greenberg LA, 'An antimony electrode for the continuous recording of the acidity of human gastric contents' *Science,* (1941) 93 479.
66. Horrocks BR, Mirkin MV, Pierce DT, Bard AJ, Nagy G, Toth K, 'Scanning Electrochemical Microscopy XIX. Ion-Selective Potentiometric Microscopy' *Anal. Chem.* (1993) 65 1213.
67. Patel BA, Bitziou E & O'Hare D, 'Simultaneous detection of pH changes and histamine release from oxyntic glands in isolated stomach' *Anal. Chem.* 80 8733–8740 (2008).
68. Bitziou E, O'Hare D & Patel BA 'Spatial changes in acid secretion from isolated stomach tissue using a pH-histamine sensing microarray' *Analyst* 135 482–487 (2010).
69. Hitchman ML, & Ramanathan S, 'Evaluation of iridium oxide electrodes formed by potential cycling as pH probes' *Analyst* 113 35(1988).
70. Yamanaka K, 'Anodically electrodeposited iridium oxide films (AEIROF) from alkaline solutions for electrochromic display devices' *Jap. J. Appl. Phys.* 28 632–37 (1989).
71. Bezbaruah AN; Zhang TC, 'Fabrication of anodically electrodeposited iridium oxide film pH microelectrodes for microenvironmental studies' *Anal. Chem.* 74 5726–5733 (2002).
72. Marzouk SAM 'Improved electrodeposited iridium oxide pH sensor fabricated on etched titanium substrates' *Anal. Chem.* 75 1258–1266 (2003).
73. Moussy F, & Harrison DJ 'Prevention of the Rapid Degradation of Subcutaneously Implanted Ag/AgCl Reference Electrodes Using Polymer Coatings' *Anal. Chem.* 66 674–679 (1994).
74. Bakker EP, Bühlmann P & Pretsch E, 'Carrier-based ion-selective electrodes and bulk optodes 1. General characteristics' *Chem. Rev.* 97 3083–3132 (1997).
75. Bühlmann P, Pretsch E & Bakker E, 'Carrier-based ion-selective electrodes & bulk optodes 2. Ionophores for potentiometric and optical sensors', *Chem. Rev.* 98 1593–1688 (1998).
76. Bakker E & Pretsch E, 'Potentiometric sensors for trace metal analysis' *TrAC Trends in Analytical Chemistry* 24 199–207 (2005).
77. Pretsch E, 'The new wave of ion-selective electrodes' *TrAC, Trends in Analytical Chemistry* 26 46–51 (2007).
78. Bobcka J, Ivaska A & Lewenstam A, 'Potentiometric ion sensors' 108 329–51 (2008).
79. Lindner E & Buck RP, 'Microfabricated potentiometric electrodes and their *in vivo* applications' *Anal. Chem.*, 72, 336A (2000).

80. Bausells J, Errachid A, Zine N, 'Biosensors based on standard dielectric materials' *Proc. Electrochem. Soc*. 2003-1 'Dielectrics in emerging technologies' 48. 2003-1, 48. (2003).
81. Wygladacz K, Durnas M, Parzuchowski, P, Brzozka, Z & Malinowska E. 'Miniaturized sodium-selective sensors based on silicon back-side contact structure with novel self-plasticizing ion-selective membranes' *Sens. Actuators, B* 95 366–372 (2003).
82. Sundfors F, Bereczki R, Bobacka J, Toth K, Ivaska A & Gyurcsányi, R. E. 'Microcavity Based Solid-Contact Ion-Selective Microelectrodes' *Electroanalysis*, *18*, 1372–8 (2006).
83. Guenat OT, Generelli S, de Rooij NF, Koudelka-Hep M, Berthiaume F & Yarmush MC, 'Development of an Array of Ion-Selective Microelectrodes Aimed for the Monitoring of Extracellular Ionic Activities', *Anal. Chem*. 78 7453–60 (2006)
84. Tymecki Ł, Zwierkowska E, Koncki R. 'Screen-printed reference electrodes for potentiometric measurements' *Anal. Chim. Acta*, 526 3–11 (2004).
85. Liao W-Y, & Chou T-C 'Fabrication of a Planar-Form Screen-Printed Solid Electrolyte Modified Ag/AgCl Reference Electrode for Application in a Potentiometric Biosensor' *Anal. Chem*. 78 4219 (2006).
86. Vazquez M, Danielsson P, Bobacka J, Lewenstam A. & Ivaska A. 'Solution-cast films of poly (3,4-ethylenedioxythiophene) as ion-to-electron transducers in all-solid-state ion-selective electrodes' *Sens. Actuators, B* 97 182 (2004).
87. Cosofret V, Erdösy M, Johnson TA, Buck RP, Ash RB, Neuman MR *Anal. Chem*. 1995, *67*, 1647–1653.
88. Lindner E, Buck R. *Anal. Chem*. 2000, 72, 336A–345A.
89. Uhlig A, Lindner E, Teutloff C, Schnakenberg U & Hintsche R 'Miniaturized ion-selective chip electrodes for sensor application' *Anal. Chem.,* 69, 4032–4038 (1997).
90. Yoon HJ, Shin JH, Lee SD, Nam H, Cha GS, Strong TD Brown RB 'Solid state ion sensors with a liquid junction-free polymer membrane-based reference electrode for blood analysis' *Sens. Actuators, B 64*, 8–14(2000).
91. Compton RG & Banks CE 'Understanding voltammetry' World Scientific Press, New Jersey, 2007.
92. Bockris JO'M, Reddy AKN 'Modern Electrochemistry Volume 2, Part 2', Plenum, New York (2000).
93. Wightman RM & Wipf DO, in Bond A (ed.) 'Electroanalytical Chemistry Volume 15' Marcel Dekker, New York 1989, p267.
94. Saito Y *Rev. Polarograph*. 15 177 (1968).
95. Bond, Luscombe AMD, Oldham KB & Zoski CG, *J. Electroanal. Chem*. 249 1–14.
96. Patel BA, Arundell M, Parker KH, Yeoman MS & O'Hare D, 'Microelectrode investigation of neuronal ageing from a single identified neurone' *Physical Chemistry Chemical Physics* 12(34) 10065–10072 (2010)
97. Amatore C, Oleinick AI, Svir A. 'Diffusion from within a Spherical Body with Partially Blocked Surface: Diffusion through a Constant Surface Area' *Chem. Phys. Chem*. 11 149 (2009); 'Reconstruction of Aperture Functions During Full Fusion in Vesicular Exocytosis of Neurotransmitters' *ib*. 159 (2009).
98. Patel BA, Arundell M, Parker KH, Yeoman MS, O'Hare D, 'Detection of nitric oxide release from single neurons in the pond snail, *Lymnaea stagnalis*' *Anal. Chem*. 78(22) 7643–7648 (2006).
99. Yeoman MS, Patel BA, Arundell M, Parker K, O'Hare D 'Synapse-specific changes in serotonin signalling contribute to age-related changes in the feeding behaviour of the pond snail, *Lymnaea*' *J. Neurochem*. 106(4) 1699–1709 (2008).
100. Phillips CG & Jansons KM, *Proc. Roy. Soc. A* 428 431–449.
101. O'Hare D, Parker KH, Winlove CP, *J. Biomed Eng* 13 304 (1991).
102. Justice JB (ed.) *Voltammetry in the Neurosciences* Humana, Clifton, New Jersey 1987.
103. Cahill PS, Walker QD, Finnegan JM, Mickelson GE, Travis ER & Wightman RMW, *Analytical Chemistry* 68 3180–3186 (1996).

104. Compton RG & Banks CE, 'Understanding Voltammetry' World Scientific, New Jersey 2007.
105. Hochstetler SE, Puopolo M, Gustincich S, Raviola E, Wightman RM, 'Real time amperometric measurements of zeptomole quantities of dopamine released from neurons', *Anal. Chem.* 72 489–496 (2006).
106. Bard AJ & Faulkner LR, *Electrochemical Methods* Wiley, New York 1980.
107. Fleming BD, Barlow NL, Zhang J, Bond AM, Armstrong FA, Application of Power Spectra Patterns in Fourier Transform Square Wave Voltammetry to Evaluate Electrode Kinetics of Surface Confined Proteins, *Anal. Chem.,* 78 2948–2956 (2006)
108. Zhang J, Bond AM, Theoretical Studies of Large Amplitude Alternating Current Voltammetry for a Reversible Surface-Confined Electron Transfer Process Coupled to a Pseudo First-Order Electrocatalytic Process, *J. Electroanal. Chem.* 600 23–34 (2007).
109. Anastassiou C, Parker KH & O'Hare D 'Determination of kinetic and thermodynamic parameters of surface confined species through ac voltammetry and a nonstationary signal processing technique: the Hilbert transform' *Anal. Chem.* 77 3357–3364 (2005).
110. Anastassiou CA, Patel BA, Parker KH & O'Hare D, 'Characterisation of ac voltammetric reaction - diffusion dynamics: from patterns to physical parameters', *Anal. Chem.* 78 4383–4389 (2006).
111. Anastassiou CA , Parker KH, O'Hare D, 'Scaling in nonstationary voltammetry representations', *J Phys. Chem. A*, 111, 13053–13060 (2007).
112. Anastassiou CA, Patel BA, Arundell M, Yeoman MS, Parker KH and O'Hare D, 'Novel subsecond voltammetric separation between dopamine and serotonin in the presence of ascorbate' *Anal. Chem.* 78(19) 6990–6998 (2006).
113. Bell CG, Anastassiou CA, O'Hare D, Parker KH & Siggers JH, Theoretical treatment of high-frequency, large-amplitude ac voltammetry applied to ideal surface-confined redox systems, *Electrochimica Acta* 64 71–80 (2012).
114. Bell CG, Anastassiou CA, O'Hare D, Parker KH , Siggers JH 'Large-amplitude ac voltammetry: Theory for reversible redox reactions in the slow scan limit approximation', *Electrochimica Acta* 56(17) 6131–6141 (2011).
115. Heer F, Franks W, Blau A, Taschini S, Ziegler C, Hierlemann A, Baltes H 'CMOS microelectrode array for the monitoring of electrogenic cells' *Biosensors and Bioelectronics* 20(2) 358–366 (2004).
116. Graham AHD, Robbins J, Bowen CR *et al.,* 'Commercialisation of CMOS Integrated Circuit Technology in Multi-Electrode Arrays for Neuroscience and Cell-Based Biosensors' *Sensors* 11(5) 4943–4971 (2011).
117. Graham AHD, Bowen CR, Surguy SM, 'New prototype assembly methods for biosensor integrated circuits' *Medical Engineering & Physics* 33(8) 973–979 (2011).
118. Graham AHD, Surguy SM, Langlois P, Bowen CR, Taylor J et al. Modification of standard CMOS technology for cell-based biosensors, *Biosensors & Bioelectronics*, 31(1) 458–462 (2012).
119. Lin Y, Trouillon R, Svensson MI, Keighron JD, Cans AS and Ewing AG, Carbon-Ring Microelectrode Arrays for Electrochemical Imaging of Single Cell Exocytosis: Fabrication and Characterization. *Anal. Chem.* 84 2949–2954 (2012).
120. Huang X-J, O'Mahony AM, & Compton RG, 'Microelectrode Arrays for Electrochemistry: Approaches to Fabrication', *Small*, 5 776–788 (2009)
121. Patel BA, Arundell M, Quek RGW, Harvey SLR, Ellis IR, Florence MM, Cass AEG, Schor AM, O'Hare D, 'Individual addressable microelectrode array for monitoring oxygen and nitric oxide release' *Anal. Bioanal. Chem.* 390(5) 1379–1387 (2008).
122. Trouillon R, Combs Z, Patel BA and O'Hare D, 'Comparative study of the effect of various electrode membranes on biofouling and electrochemical measurements' *Electrochem. Comm.* 11 1409–1413 (2009).
123. Frost M & Meyerhoff ME, '*In vivo sensors: tackling biocompatibility*' *Anal. Chem.* 78 7370–7377 (2006).

124. Morais JM, Papadimitrakopoulos IF, and Burgess DJ 'Biomaterials/Tissue Interactions: Possible Solutions to Overcome Foreign Body Response' *American Association of Pharmaceutical Scientists J*. 12 188–196 (2010).
125. Ward WK, Quinn MJ, Wood MD, Tiekotte KLr, Sudha Pidikiti, Jennifer A. Gallagher *Biosensors 7 Bioelectronics* 19 155–163 (2003) 'Vascularizing the tissue surrounding a model biosensor: how localized is the effect of a subcutaneous infusion of vascular endothelial growth factor (VEGF)?'
126. Klueh U, Dorsky DI, Kreutzer DL, 'Enhancement of implantable glucose sensor function in vivo using gene transfer-induced neovascularization' *Biomaterials* 26 1155–63 (2005).
127. Trouillon R, Cheung C, Patel BA & O'Hare D, 'Comparative study of poly(styrenesulphonate)/poly(L-lysine) and fibronectin as biofouling-preventing layers in dissolved oxygen electrochemical measurements' *Analyst* 134 784–93 (2009).
128. Ressinea A, Vaz-Domínguez C, Fernandez VM, De Lacey AL, Laurell T, Ruzgas T, Shleev S 'Bioelectrochemical studies of azurin and laccase confined in three-dimensional chips based on gold-modified nano-/microstructured silicon' *Biosensors and Bioelectronics* 25 1001–1007 (2010).
129. Trasatti S and Petriim OA 'Real surface area measurements in electrochemistry' *Pure & Appl. Chem.,* 63, 71 1–734 (1991)
130. Trouillon R, Kang, D-K, Park H, Chang S-I & O'Hare D, 'Angiogenin induces nitric oxide synthesis in endothelial cells by PI-3 kinases and nuclear translocation pathways' *Biochemistry* 49 3282–3288 (2010).
131. Trouillon R, Cheung C, Patel BA, O'Hare D, 'Electrochemical study of the intracellular transduction of vascular endothelial growth factor induced nitric oxide synthase activity using a multi-channel biocompatible microelectrode array' *Biochim. Biophys. Acta (Gen. Subj.)*, 1800(9) 929–936 (2010).
132. Trouillon R, Williamson ED, Saint RJ, O'Hare D, 'Electrochemical detection of the binding of *Bacillus anthracis* protective antigen (PA) to the membrane receptor on macrophages through release of nitric oxide' *Biosensors and Bioelectronics* 38 138–144 (2012).
133. Patten HV, Meadows KE, Hutton LA, Iacobini JG, Battistel D, McKelvey K, Colburn AW, Newton ME, Macpherson JV, and Unwin PR, 'Electrochemical Mapping Reveals Direct Correlation between Heterogeneous Electron-Transfer Kinetics and Local Density of States in Diamond Electrodes' Angew. Chem. Int. Ed. 51, 7002–7006 (2012)
134. Trouillon R & O'Hare D 'Comparison of glassy carbon and boron doped diamond electrodes: resistance to biofouling' *Electrochimica Acta* 55(22) 6586–6595 (2010).
135. Trouillon R, O'Hare D, Einaga Y, 'Effect of doping level on the biological stability of hydrogenated boron doped diamond electrodes' *Physical Chemistry Chemical Physics* 13 5422–5429 (2011).
136. Park J, Quaiserova-Mocko V, Patel BA, Novotny M, Liu A, Bian X, Galligan JJ, Swain G M 'Diamond microelectrodes for in vitro electroanalytical measurements: current status and remaining challenges' *Analyst*, 133 17–24 (2008).
137. Park J, Show Y, Quaiserova V, Galligan JJ, Fink GD, Swain GM, 'Diamond microelectrodes for use in biological environments' *J. Electroanal. Chem*. 583 56–68 (2005).
138. Patel BA 'Electroanalytical approaches to study signaling mechanisms in the gastrointestinal tract' *Neurogastroenterlogy & Motility* 23 595–605
139. Hutton LA, Iacobini JG, Bitziou E, Channon RB, Newton ME, Macpherson JV, 'Examination of the factors affecting the electrochemical performance of oxygen-terminated polycrystalline boron-doped diamond electrodes' *Anal. Chem.* in press dx.doi.org/10.1021/ac401042t|A.
140. Jones CP, Jurkschat K, Crossley A, Compton RG, Riehl BL, Banks CE, 'Use of high-purity metal-catalyst-free multiwalled carbon nanotubes to avoid potential experimental misinterpretations' *Langmuir*, 23 9501–9504 (2007).
141. Sims MJ, Rees NV, Dickinson EJF, Compton RG, 'Effects of thin-layer diffusion in the electrochemical detection of nicotine on basal plane pyrolytic graphite (BPPG) electrodes modified with layers of multi-walled carbon nanotubes (MWCNT-BPPG)' *Sensors and Actuators B*, 144, (2010), 153–158.

142. Dumitrescu I, Unwin PR, and Macpherson JV, 'Electrochemistry at Carbon Nanotubes: Perspectives and Issues' *Chem. Commun*., 45, 6886–6901 (2009).
143. P. Bertoncello JP, Edgeworth JV, Macphersonand Unwin PR 'Trace level cyclic voltammetry facilitated by single-walled carbon nanotube network electrodes' *J. Am. Chem. Soc*. 129 10982–10983 (2007).
144. Güell AG, Meadows KE, Unwin PR, and Macpherson JV, 'Trace voltammetric detection of serotonin at carbon electrodes: comparison of glassy carbon, boron doped diamond and carbon nanotube network electrodes' *Phys. Chem. Chem. Phys*. 12 10108–10114 (2010).
145. Dudin PV, Snowden ME, Macpherson JV, and Unwin PR 'Electrochemistry at nanoscale electrodes (NSEs): individual single walled carbon nanotubes (SWNTs) and SWNT-templated metal nanowires' *ACS Nano*, 5 10017–10025 (2011)
146. Boero C, Carrara S, de Micheli G 'Long-term Biosensors for Metabolite Monitoring by using Carbon Nanotubes' *Sensors & Transducers Journal,* 125, , 229–237 (2011).
147. Brownson DAC, Kampouris DK, Banks CE, 'Graphene electrochemistry: fundamental concepts through to prominent applications' *Chem. Soc. Rev.,* 41 6944–6976 (2012).
148. Kim YJ, Chun S-E, Whitacreab J & Bettinger CJ, 'Self-deployable current sources fabricated from edible materials' *J. Mater. Chem. B* DOI: 10.1039/c3tb20183j in press.
149. Grande, Chundi L, Wei VT, Bower D, Andrew C, P, Ryhanen, T , 'Graphene for energy harvesting/storage devices and printed electronics' *Particuology* 10 1–8 (2012)
150. Xuan Y, Sandberg M, Berggren M, Crispin X, *Organic Electronics* 13 632–637 (2012).
151. Kawahara J, Andersson Ersman P, Nilsson D, Katoh K, Nakata Y, Sandberg M, Nilsson M, Gustafsson G & Berggren M, 'Flexible active matrix addressed displays manufactured by printing and coating techniques' *J. Polym. Sci. B Polym. Phys*. 51 265–271 (2013).
152. http://www.nano-tera.ch/news/#anchor50